Available online at www.sciencedirect.com
ScienceDirect
Biochimica et Biophysica Acta 1773 (2007) 1511–1525
Biochimica et Biophysica Acta BBA
www.elsevier.com/locate/bbamcr

Three autocrine feedback loops determine HIF1α expression in chronic hypoxia

Amina A. Qutub *, Aleksander S. Popel

Department of Biomedical Engineering, School of Medicine, Johns Hopkins University, 613 Traylor Building, 720 Rutland Avenue, Baltimore, MD 21205, USA

Received 8 February 2007; received in revised form 13 June 2007; accepted 12 July 2007
Available online 20 July 2007

Abstract

Hypoxia occurs in cancer, prolonged exercise, and long-term ischemia with durations of several hours or more, and the hypoxia-inducible factor 1 (HIF1) pathway response to these conditions differs from responses to transient hypoxia. We used computational modeling, validated by experiments, to gain a quantitative, temporal understanding of the mechanisms driving HIF1 response. To test the hypothesis that HIF1α protein levels during chronic hypoxia are tightly regulated by a series of molecular feedbacks, we took into account protein synthesis and product inhibition, and analyzed HIF1 system changes in response to hypoxic exposures beyond 3 to 4 h. We show how three autocrine feedback loops together regulate HIF1α hydroxylation in different microenvironments. Results demonstrate that prolyl hydroxylase, succinate and HIF1α feedback determine intracellular HIF1α levels over the course of hours to days. The model provides quantitative insight critical for characterizing molecular mechanisms underlying a cell's response to long-term hypoxia.

Keywords: Angiogenesis; Cancer; Chronic hypoxia; Computational modeling; Ischemia; Prolonged exercise

1. Introduction

Hypoxia occurs in cancer, prolonged exercise, and long-term ischemia with durations of several hours or more. Under these conditions, the threshold of hypoxic response changes. Mammalian cells exposed to chronic hypoxia (5% oxygen), and then exposed to a lower level of oxygen (0.5%) are capable of showing a response consistent with acute hypoxia, but attenuated [1]. In addition, mammals in normoxia, with prior chronic hypoxic exposure, exhibit an augmented ventilatory response to subsequent acute hypoxia [2]. Furthermore, hypoxic preconditioning contributes to a limited hypoxic response in reoxygenated cells [3] and shows protective effects in mammals exposed to ischemia [4]. Hydroxylation enzyme synthesis and its effect on degradation of hypoxia inducible factor 1 α (HIF1α) contribute to this setpoint adjustment [1,3,5,6]. Here we sought to explore in depth the dynamics of this process, and test the hypothesis that three feedback loops (HIF1α synthesis, prolyl hydroxylase synthesis and succinate (SC) production inhibition) work in combination to tightly regulate the effects of chronic hypoxia via control of HIF1α degradation.

HIF1 is a heterodimer, comprised of subunits HIF1α and HIF1β. The beta subunit is constitutively expressed in cells. Expression of the alpha subunit may be induced by a number of pathways, and its degradation is highly sensitive to O_2 levels. Called a 'master switch for hypoxic gene expression' [7,8], intracellular HIF1α in normoxia is experimentally undetectable; during hypoxia, it rapidly accumulates in the cell nucleus, and triggers gene expression. In normoxia, enzymes called prolyl hydroxylase domains (PHDs) react with HIF1α (Fig. 1A). PHDs hydroxylate HIF1α at the HIF1α protein's two proline residue sites Pro-402 and Pro-564, in the oxygen-dependent degradation domain. The activity of PHDs depends on the amount of oxygen available. One of the PHD isoforms, PHD2, is the most abundant prolyl hydroxylase isoform in the cell cytoplasm during normoxia; it has been credited as a controller of steady-state HIF1α concentrations under these conditions in a range of cell types [9,10]. Following the reaction with PHD, the hydroxylated HIF1α is free to bind to a von Hippel-Lindau (VHL) ubiquitin ligase complex (VHL in this paper refers to the protein product

Abbreviations: HIF, hypoxia-inducible factor; PHD, prolyl hydroxylase domain; SC, succinate; SDH, succinate dehydrogenase; VHL, von Hippel-Lindau; Asc, ascorbate; 2OG, 2-oxoglutarate; ARNT, aryl hydrocarbon receptor nuclear translocator

* Corresponding author. Tel.: +1 410 955 1787.
E-mail address: aqutub@jhu.edu (A.A. Qutub).

0167-4889/$ - see front matter © 2007 Elsevier B.V. All rights reserved.
doi:10.1016/j.bbamcr.2007.07.004

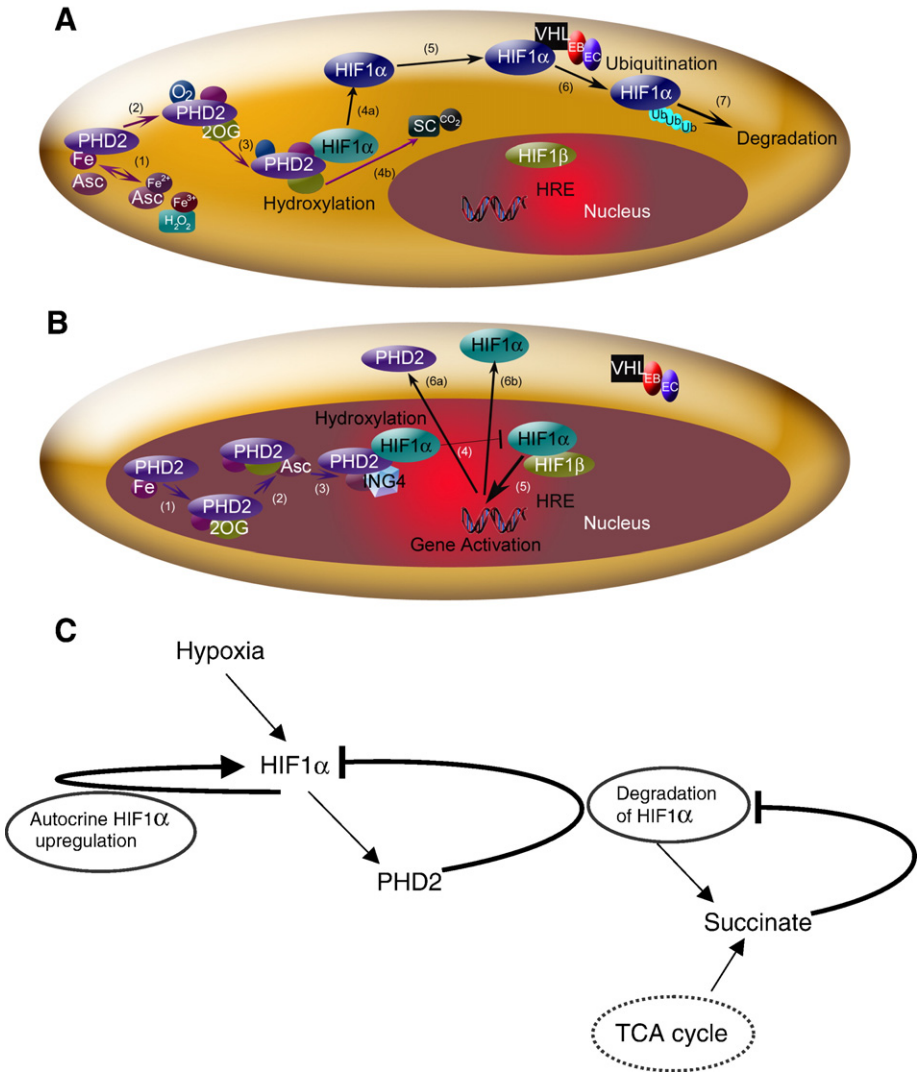

Fig. 1. The HIF1 pathway in normoxia (A) and hypoxia (B). (A) HIF1α hydroxylation and degradation in the presence of oxygen involves: (1) the independent oxidation–reduction reactions of ascorbate (Asc) and iron (Fe); (2) and (3) prolyl hydroxylase 2 (PHD2) binding to Fe, 2-oxoglutarate (2OG), and O_2; (4a) PHD2 hydroxylation of HIF1α, involving (4b) production of the by-products succinate and CO_2; (5) unbound hydroxylated HIF1α moving in the cell cytoplasm; (6) the von Hippel-Lindau (VHL)–Elongin B (EB)–Elongin C (EC) complex ubiquitinating HIF1α; and (7) HIF1α degradation. A color change in HIF1α indicates addition of a hydroxyl group. (B) In hypoxia, HIF1α enters the nucleus, where hydroxylation, but no degradation occurs. (1) and (2) PHD2 binding to Fe, 2OG and Asc, but not O_2. (3) The protein inhibitor of growth 4 (ING4) binding to PHD2 may regulate HIF1α transcriptional activity and (4) block HIF1α-HIF1β binding. (5) When HIF1α-HIF1β binding occurs, the HIF1 dimer can transcriptionally activate genes at the hypoxia response element (HRE) site. Activated HIF1-dependent genes, where protein levels are upregulated, include PHD2 (6a) and HIF1α (6b). (C) Schematic of a potential mechanism for adaptation during chronic hypoxia. Three feedback loops govern HIF1α hydroxylation; HIF1α synthesis; prolyl hydroxylase 2 (PHD2) synthesis; and succinate production inhibition. Succinate is also a metabolic product of the TCA cycle.

of the VHL gene; this also is known as pVHL), which tags HIF1α for proteasomal destruction.

In hypoxia, HIF1α escapes hydroxylation, accumulates and enters the cell nucleus, where it binds to HIF1β (known also as ARNT, aryl hydrocarbon receptor nuclear translocator) (Fig. 1B). The HIF1α-HIF1β dimer transcriptionally activates a host of genes, including those encoding for angiogenic growth factors [11–13]; erythropoietin [14]; and proteins critical to glycolysis [15]. Through transcriptional regulation of these genes, HIF1 contributes to angiogenesis and altered cell metabolism — critical processes that facilitate a tumor's growth or help extend muscle contraction, for example. HIF1 and its related pathways are attractive therapeutic targets in cancer and ischemia [16,17], and are measures of enhanced exercise response [18]. Specific to this work, HIF1 regulation offers a way to alter physiological responses to the chronic ischemia found in peripheral vascular disease and coronary artery disease [19] and the long-term, heterogeneous hypoxia found in different tumors [20,21].

A balance of HIF1α levels and HIF1α activity seems necessary to achieve health [22,23]. This is particularly relevant in conditions of chronic hypoxia, where continued upregulation of hypoxia-induced genes may induce or predispose individuals to malignancy [24]. In vitro studies have shown how the hypoxic response varies based on vascular microenvironment [25,26]. Exposure to low levels of oxygen for over 3 h can alter HIF1α hydroxylation, and thereby HIF1 signaling, through multiple pathways.

Table 1
Model variables and their abbreviations

Variable	Abbreviation
Concentration of A	[A]
AEB	Binding of A and B
Ascorbate	Asc
Iron	Fe^{2+}, Fe^{3+}
Prolyl hydroxylases	PHD2
Hypoxia inducible factor hydroxylated	$HIF1\alpha_h$
HIF1α unhydroxylated	HIF1α
von Hippel Lindau	VHL
Succinate	SC
Succinate dehydrogenase	SDH
Carbon dioxide	CO_2
2-oxoglutarate	2OG
Oxygen	O_2
Elongin B	EB
Elongin C	EC
Cullins 2	Cul2
Hydrogen peroxide	H_2O_2
Dehydro-ascorbate	dehydroAsc
Start time for HIF1α synthesis (h)	$t_{HIF1\alpha}$
Start time for PHD2 synthesis (h)	t_{PHD2}
Reverse rate for PHD2 complex binding to HIF1α (min^{-1})	$k_{off,HIF1\alpha}$
Reverse rate for PHD2 complex binding to HIF1α, incorporating SC (min^{-1})	$k'_{off,HIF1\alpha}$
Kinetic term relating O_2 to SC levels (min^{-1})	k_{SC}
Production constant for HIF1α (μM min^{-1})	$k_{prod,HIF1\alpha}$
Production constant for HIF1α (min^{-1})	$k'_{prod,HIF1\alpha}$
Production constant for PHD2 (unitless)	$k_{prod,PHD2}$
Production constant for PHD2 (unitless)	$k'_{prod,PHD2}(t)$
Synthesis term for HIF1α (μM min^{-1})	$q_{prod,HIF1\alpha}$
Synthesis term for PHD2 (μM min^{-1})	$q_{prod,PHD2}$
Synthesis term for PHD2 (μM min^{-1}), case 2	$q1_{prod,PHD2}$
Synthesis term for PHD2 (μM min^{-1}), case 2	$q2_{prod,PHD2}$

Three mechanisms altering hydroxylation by PHD2 and HIF1α levels include autocrine upregulation of HIF1α activity by HIF1α synthesis, downregulation of HIF1α by PHD2 synthesis, and succinate production inhibition. Knowledge of HIF1α and PHD2 synthesis comes from in vitro studies and limited in vivo experiments showing PHD2 is HIF1-dependent and hypoxia-inducible [3,5,27,28]. In vivo experiments in neonatal rat brain have also shown that HIF1α and PHD2 synthesis occur at different times in response to hypoxic preconditioning [6]. PHD2 hydroxylation of HIF1α produces the compound succinate. Succinate and 2-oxoglutarate (2OG), a PHD2 cofactor, act competitively, and succinate thereby feedback inhibits the PHDs [22,23,29]. Succinate dehydrogenase (SDH), a mitochondrial membrane enzyme, oxidizes succinate; and inhibiting SDH can lead to intracellular succinate levels near 0.5 mM [23]. Here, we show how in chronic conditions, the three feedback loops can combine to determine HIF1α hydroxylation, intracellular HIF1α protein levels, and ultimately, intracellular hypoxic adaptation.

2. Methods

2.1. Formulation of Computational Model

The biochemical pathway model of oxygen sensing by HIF1α was introduced elsewhere [30]. Here we extend the model by adding succinate and its associated molecules, and further characterizing hypoxia-induced synthesis of HIF1α and PHD2. Briefly, from a comprehensive analysis of experimental data, we represent the hydroxylation of HIF1α by PHDs and the ubiquitination of hydroxylated HIF1α by VHL (Fig. 1A). We modeled the hydroxylation of HIF1α by PHD2 in the cell cytoplasm. The compounds involved in binding to PHD2 in preparation for the hydroxylation of HIF1α include iron, 2-oxoglutarate, oxygen and ascorbate (Asc). The modified PHD2 then binds and hydroxylates HIF1α. Simultaneously, the hydroxylation reaction produces the by-products succinate and carbon dioxide. Hydroxylated HIF1α is recognized and ubiquitinated by VBC (VHL·Elongins BC), the complex that includes VHL bound to Elongins B and C, Cul2 and Rbx1. Table 1 lists the compounds included in the model.

Eq. (1) describes the overall scheme of HIF1α degradation. The model includes HIF1α hydroxylation, independent reactions of iron and ascorbate, succinate accumulation and product inhibition (Eqs. (A1), (A2), and (A5)), PHD2 synthesis (Eq. (A1)), HIF1α synthesis (Eq. (A2)), and the binding of HIF1α to VHL (Eqs. (23–26) in [30]) illustrated in Fig. 1A–C.

$$\begin{array}{l} PHD2 + Fe^{2+} + 2OG + O_2 + Asc \leftrightarrow \\ \qquad\qquad \curvearrowright \\ PHD2 \cdot Fe^{2+} \cdot 2OG \cdot O_2 \cdot Asc \leftrightarrow PHD2 + succinate + CO_2 \\ \qquad\qquad \curvearrowright \\ HIF1\alpha \qquad HIF1\alpha_{hydroxylated} \end{array} \tag{1}$$

The hydroxylation reactions follow enzyme–substrate binding kinetics. Governing equations are determined from mass balances surrounding the substrate and the intermediate enzyme–substrate complexes. A combination of

Table 2
Parameters and their initial values for the degradation of HIF1α in normoxia, and accumulation of HIF1α and PHD2 in hypoxia

Constant	Value	Reference
$[H_2O_2]_0$	0.20 μM [a]	[75]
$[O_2]_0$	200 μM	[37]
$[Fe^{3+}]_0$	0 μM	–
$[Fe^{2+}]_0$	50 μM	[37]
$[2OG]_0$	1000 μM	[37]
$[Asc]_0$	1000 μM	[37]
$[HIF1\alpha]_0$	1 μM	[37]
$[PHD2]_0$	1 μM; 4 nM (where stated for in vitro comparisons)	[37]
	0.15 μM (calculated by model to scale with experiment)	[5]
$[SC]_0$	0.5 μM (0–5 mM) [b]	[23,36,69]
$k_{off,HIF1\alpha}$	0.7 min^{-1}, estimate	–
$k'_{off,HIF1\alpha}$	>0.7 min^{-1}, $k'_{off,HIF1\alpha}=k_{off,HIF1\alpha}+k_{on,SC}$	–
k_{SC}	0.0001–0.1 min^{-1}, range explored	–
$k_{prod,HIF1\alpha}$	0.01–1 μM h^{-1}, range explored	–
$k'_{prod,HIF1\alpha}$	0.1 or 1 h^{-1}	–
$k_{prod,PHD2}$	C_3 $k_{prod,HIF1\alpha}$, unitless (relative to HIF1α synthesis) where C_3=0–1000 (fold times $k_{prod,H\alpha}$) $\mu M^{-1}\cdot h$	–
$k'_{prod,PHD2}$	$C_4 \cdot$ time, unitless (relative to HIF1α synthesis) where C_4=0.01 h^{-1}	[5] [c]
$t_{HIF1\alpha}$	3 h	[5]
t_{PHD2}	4 h	[5]

Values are experimentally determined or estimated, or estimated from model calculations as noted. All values are at 37 °C.

[a] Assumed, as an approximation. Range of 0.13–0.25 μM given in the cited reference. Within this range, the effects on varying H_2O_2 initial concentration on the model response are small.

[b] Initial intracellular concentration for succinate is not zero, but a base value due to Krebs cycle succinate production. For the purposes of product inhibition of the HIF1α hydroxylation, all succinate considered is formed by the hydroxylation reaction.

[c] Approximate C_4 value estimated from slope of curve for PHD2 protein levels vs. time at 1% O_2 from reference [6].

Table 3
Tested models of HIF1α and PHD2 synthesis in chronic hypoxia

Model	Value	Equation	Time equation begins
Case 1	$q_{\text{prod,HIF1}\alpha}$	$k_{\text{prod,HIF1}\alpha} \cdot \frac{[O_2]}{([O_2]+C_2)}$ where $C_2=0.01$ μM, unless stated otherwise	$t_{\text{HIF1}\alpha}=3$ hrs
	$q_{\text{prod,PHD2}}$	$k_{\text{prod,PHD2}} \cdot q_{\text{prod,HIF1}\alpha}$	$t_{\text{PHD2}}=4$ hrs
Case 2	$q_{\text{prod,HIF1}\alpha}$	$k_{\text{prod,HIF1}\alpha} \cdot \frac{[O_2]}{([O_2]+C_2)}$ where $C_2=0.01$ μM, unless stated otherwise	$t_{\text{HIF1}\alpha}=3$ hrs
	$q_{\text{prod,PHD2}}$	$k'_{\text{prod,PHD2}}(t) \cdot k_{\text{prod,PHD2}} \cdot q_{\text{prod,HIF1}\alpha}$	$t_{\text{PHD2}}=4$ hrs (ends at 24 hrs)
	$q_{\text{prod,PHD2}}$	$k_{\text{prod,PHD2}} \cdot q_{\text{prod,HIF1}\alpha}$	$t_{\text{PHD2}}=24$ hrs
Case 3	$q_{\text{prod,HIF1}\alpha}$	$k'_{\text{prod,HIF1}\alpha} \cdot \frac{[O_2]\cdot[\text{HIF1}\alpha]}{([\text{HIF1}\alpha]+C_1\cdot[O_2]}$ where $C_1=0.01$ or 1, as stated (unitless)	$t_{\text{HIF1}\alpha}=3$ hrs
	$q_{\text{prod,PHD2}}$	$k_{\text{prod,PHD2}} \cdot q_{\text{prod,HIF1}\alpha}$	$t_{\text{PHD2}}=4$ hrs

The form of each equation is estimated from experimental data on time and oxygen dependency of synthesis. Available cellular oxygen concentration $[O_2]$ is constant throughout all model simulations, except where it is a function of succinate, as noted.

enzyme–substrate saturation assumptions was used for the binding of iron, ascorbate, 2-oxoglutarate and oxygen to PHD2, PHD2 hydroxylation of HIF, and VHL-mediated ubiquitination. In the hydroxylation reaction of PHDs with HIF1, we represented the binding of PHD2 with the substrates iron, 2-oxoglutarate and oxygen, sequentially; redox reaction for ascorbate and iron are included as separate equations [30]. These hydroxylation steps and their output were validated against experiments previously [30]. Recent assays further confirm the relationship of PHD2 activity and oxygen, as well as qualitatively, concur with the model on the effects of ascorbate [31]. Model inputs are initial compound concentrations, including cellular O_2 levels (Table 2). Output is HIF1α levels in the cell cytoplasm. The described kinetic model can be found in the , Eqs. (A1) (A2) (A3) (A4) (A5) (A6); the complete model includes Eqs. (A1) (A2) (A3) (A4) (A5) (A6) and all previously studied reactions [30].

Three feedback loops hypothesized to govern HIF1 levels and thereby determine the response to chronic hypoxia are represented (Fig. 1C). Production terms are included for the synthesis of PHD2 (Eq. (A1)) and HIF1α (Eq. (A2)). Production terms $q_{\text{prod,PHD2}}$ for PHD2 in Eq. (A1) and $q_{\text{prod,HIF1}\alpha}$ for HIF1α in Eq. (A2) are nonzero only in chronic hypoxia (after 3 h, $q_{\text{prod,HIF1}\alpha}>0$; after 4 h, $q_{\text{prod,PHD2}}>0$). Estimates of these functions are based on experiments [3,5,9,32]. Product inhibition by succinate is included by modifying the backward kinetic rates for the PHD2 complex binding to unhydroxylated HIF1α (Eq. (A3)).

2.1.1. Production of HIF1α and PHD2

Several forms for the synthesis term were tested in the model ([Table 2]). It is possible that HIF1α synthesis has no inherent limit, except as a function of oxygen concentration (Cases 1 and 2, Table 3); in these cases, PHD2-dependent degradation alone causes a drop in HIF1α expression. The form of the equation in Case 1 differs from Case 2 by a function of time, and in Case 2, the PHD2 synthesis term until 24 h is time-dependent, based on experimental comparisons [5].

However, a likely possibility is that HIF1α synthesis itself has an internal limit — either as a function of limited energy to synthesize new protein or product inhibition (Case 3, Table 3). In this case, the production can be modeled using saturation kinetics as a function of HIF1α levels. Case 3 represents HIF1α synthesis (and thereby PHD2 synthesis) as a non-linear function of O_2, with a maximum at 0.5% oxygen, and decreasing synthesis at greater or lesser oxygen concentrations (Fig. 2A and B). For Cases 1 and 2, HIF1α synthesis increases monotonically as a function of O_2 (Fig. 2C and D). Effects on HIF1α hydroxylation of changing the constant C_1 in Case 3 are shown (Fig. 2E).

2.1.2. Succinate and product inhibition

In the hydroxylation reaction, PHD2 simultaneously splits oxygen to hydroxylate HIF1α, and oxidizes and decarboxylates 2-oxoglutarate to succinate (Eqs. (A1), (A2) and (A3)) [23]. Succinate and 2-oxoglutarate are also intermediate products in the citric acid (TCA) cycle. Downregulation of succinate dehydrogenase, an enzyme that degrades succinate, leads to intracellular succinate accumulation, HIF1α stabilization and HIF activation [23]. Through in vitro and in vivo experimental observations, succinate was hypothesized to act as a product inhibitor of the PHD hydroxylation reaction of HIF1α [23,33]. Product inhibition could result from 2-oxoglutarate (2OG) being converted into a succinic acid salt or succinate,[1] and therefore not allowing 2OG to be available to the PHD2 forward hydroxylation reaction. Inhibition could also result from a direct increase in the reverse flux. Alternately, it could result from binding of succinate to the PHD2 enzyme and decreasing the affinity of the enzyme for HIF1α. As the mechanism or combination of mechanisms is still being explored, we choose to represent succinate product inhibition as changes in the reverse kinetic rate (Eq. (A5)).

Intracellular levels of succinate, while yet unknown in vivo, are anticipated to vary widely by cell type and metabolic conditions [23,34,35]. The range of explored initial succinate concentrations, 0–5 mM, was determined by assuming no initial accumulation of the product for the minimum value and using in vitro levels for the maximum ([Table 2]). The maximum value of 5 mM succinate is from experiments exploring SDH and succinate activity, where succinate was added to the media of HEK293 human embryonic kidney cell extracts [23] or isolated rat liver mitochondria [36], respectively. In vivo, intracellular succinate levels would be anticipated to be lower, even in SDH dysfunction. One in vitro study estimated ~500 μM succinate is produced in cells, where SDH was inhibited [23]. A following study reported 0.1 to 1 mM succinate levels are required to inhibit PHD activity; and it was suggested that in vivo, other factors may sensitize PHD to small changes in succinate concentrations [29].

2.1.3. Calculation of intracellular oxygen for In Vivo analogies

Previously, it was assumed that reported in vitro O_2 levels could be converted to O_2 concentration in cell culture media, and this represented available cellular oxygen [30,37]. A more detailed analysis allows better approximations to intracellular O_2 levels and a direct analogy to in vivo conditions. The analysis was done by applying Fick's law of diffusion to a simulated two-dimensional cell culture layer and parameters estimated from experiments [38–41]. A related diagram and the resulting estimates for intracellular O_2 concentrations are shown in Supplemental Fig. 1. In this analysis, the culture medium acts as a barrier to oxygen diffusion. For comparison to experiments, O_2 levels provided in units of mmHg and percentages were converted to micromolal units, consistent with the previous model and as estimated in literature based on the solubility of oxygen in water [37]; 1 μM ≈ 0.78 mm Hg.

Constant O_2 supply, refreshed media and a steady-state system were assumed. O_2 consumption by a confluent cell monolayer was estimated as 2 μmol/10^7 cells/h for T47D human breast cancer cell line [42]. (While estimated as constant, this O_2 consumption depends on cell line, cell size, culture conditions, and cell confluency; a value of 4.5 μmol/10^7 cells/h for MCF7 human breast adenocarcinoma line was also previously reported [43]). With this O_2 consumption rate $R_{\text{metabolic}}$, an oxygen diffusivity through cell culture media of $D_{\text{oxy}}=2\times10^{-5}$ cm^2/s and a height (h) of 2 mm for the cell media layer [38], the steady-state value for O_2 concentration at the cell membrane–liquid interface $C_{\text{monolayer}}$ could be calculated for given atmospheric O_2 levels C_{surface} from the mass balance equation:

$$D_{\text{oxy}}(C_{\text{surface}} - C_{\text{monolayer}})/h - R_{\text{metabolized}} = 0 \quad (2)$$

For a confluent cell layer of thickness d and cell diffusion coefficient for oxygen D_{cell}, and metabolic rate $M_{\text{metabolic}}=R_{\text{metabolic}}/d$, solving the diffusion equation in the cell layer with the boundary conditions $C=C_{\text{monolayer}}$ at $x=0$; and $dC/dx=0$ at $x=d$, we obtain for C_{min}, the O_2 concentration at the bottom of the cell layer (i.e., the minimum oxygen concentration expected intracellularly):

$$C_{\text{min}} = C(x=d) = c_{\text{monolayer}} - \frac{Md^2}{2D_{\text{cell}}} \quad (3)$$

[1] 2OG ↔ succinate semialdehyde + CO_2 succinate semialdehyde + $NAD(P)^+$ + H_2O → SC + NAD(P)H.

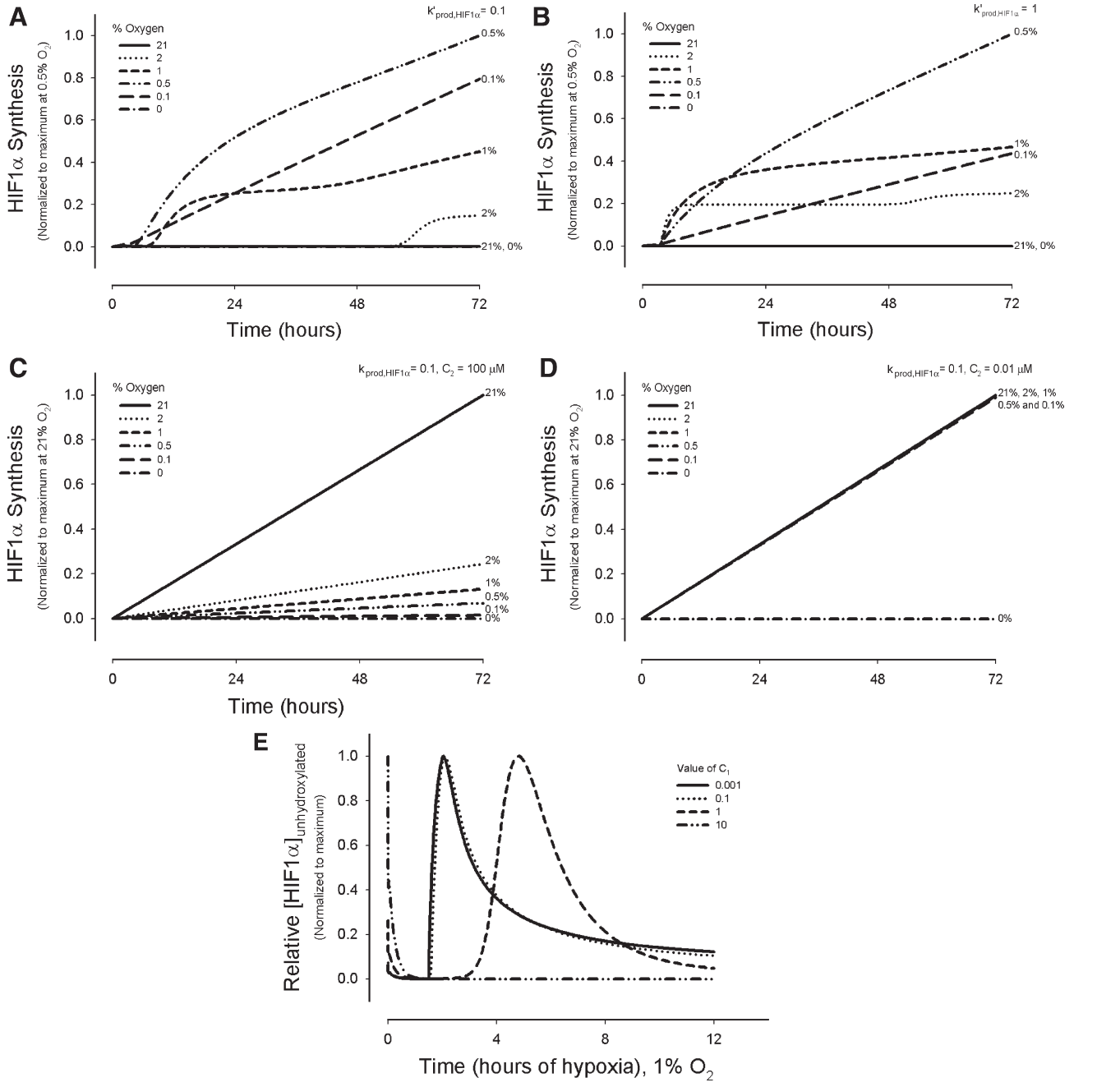

Fig. 2. HIF1α synthesis in the model as a function of time and oxygen concentrations. HIF1α synthesis term for the default model case shows how maximum HIF1α synthesis occurs at an intermediate oxygen level, while synthesis tapers at O_2 concentrations above and below 0.5%, where $k'_{prod,HIF1\alpha}=0.1$ (A) and $k'_{prod,HIF1\alpha}=1$ (B). For the other two cases, HIF1α synthesis increases linearly with time, and increasing oxygen concentrations. (C) $k_{prod,HIF1\alpha}=0.1$; $C_2=100$ μM. (D) $k_{prod,HIF1\alpha}=0.1$; $C_2=0.01$ μM. (E) Effect of changing the term C_1 in the default model, where C_1 is the constant term in the synthesis equations for HIF1α or PHD2 (Table 3, Case 3).

Cell confluency was approximated as 10^5 cells/cm^2 [38,42]. Using $d=20$ μm, $D_{cell}=10^{-5}$ cm^2/s, results are shown in Supplemental Fig. 1.

For atmospheric O_2 levels above 7%, the calculated intracellular O_2 concentration is linearly dependant on atmospheric oxygen, and calculations could be directly compared to experiments [41]. For atmospheric O_2 levels below 7%, the model estimated nearly anoxic intracellular levels, and experimental values from literature were sought for comparison.

The relationship between extracellular and intracellular O_2 levels at low O_2 concentrations is a complex function of microenvironment, cell type, and cell adaptation. Notably, intracellular respiration and O_2 consumption decrease at very low O_2 levels. Isolated mitochondria change respiratory function at intracellular O_2 levels below 1 μM or ~0.1% [44], while intact cells change O_2-dependent metabolism at a significantly higher O_2 level [45]. Respiratory changes have been shown for platelets below O_2 levels of 2.5 μM, dropping to zero O_2 consumption near 0.13 μM [46]; and for other cell types, respiratory changes occur at O_2 levels near 14–25 μM [47,48]. Furthermore, 4% atmospheric oxygen values yielded pericellular O_2 as low as 0.31% O_2 [42]. The above experimental data on O_2 consumption, while variable, was used to estimate alternate possible intracellular O_2 levels as a function of atmospheric O_2 (Supplemental Fig. 1B, dashed lines). For atmospheric O_2 levels below 7% O_2, $R_{metabolic}$ decreases as a function of limited O_2, and an approximation of a saturation curve replaces $R_{metabolic}$ in Eq. (2). Respiration rate was approximated using a K_m for oxygen of 1.8 μM, as reported for hepatocytes [49]. This assumption of decreasing metabolism is also in agreement with the observed

closeness of extracellular and intracellular O_2 levels at low O_2 levels from other studies [50].

Overall, this analysis, showing possible minimum intracellular O_2 levels with constant and with variable O_2 consumption, provides an estimate of in vivo O_2 levels for conditions described in this paper. Where this paper refers to normoxia or ~15 to 21% O_2 atmospheric levels, the approximated intracellular oxygen level is ~9 to 15%, respectively, for an O_2 consumption rate of 2 μmol/10^7 cells/h.

2.1.4. Model parameters

Default values for kinetic constants and initial conditions are shown in Table 2 with references. Ten of the kinetic terms from the original hydroxylation model and estimated ranges for the new succinate constants are derived from experimental data. Values for the synthesis kinetic rates ($k_{prod,HIF1\alpha}$, $k'_{prod,HIF1\alpha}$, $k'_{prod,PHD2}$ and $k_{prod,PHD2}$) were explored relative to one another, and their effects on the synthesis terms for model Cases 1–3 were compared (Supplement Fig. 2). Values for the unknown parameters were estimated as described in a previous study [30].

2.1.5. Numerical solution

The system of nonlinear differential equations presented in Appendix I was solved using Mathworks Matlab software. The ode23s solver, based on a modified Rosenbrock formula, was used to find a solution for the series of seventeen differential equations. For the time integration, the solver used adjustable time steps with default absolute error tolerance in the solution of 10^{-6}.

3. Results

3.1. Chronic Hypoxia: HIF1α and PHD2 synthesis

HIF1α's half-life upon reoxygenation depends on duration of hypoxic exposure. Beyond 3 h of hypoxia, synthesis of HIF1α protein occurs [9], and PHD mRNA levels are upregulated by 4 h (PHD2 minimally; PHD3 strongly [51]). mRNA levels increase for HIF1α and PHD2 followed several hours later by elevated protein expression. HIF1-dependent PHD2 protein production becomes detectable between 4 and 8 h of hypoxia in vitro, continuing beyond 24 h [5,52]. Fig. 3 shows the variability of HIF1α hydroxylation under conditions of chronic hypoxia, where a synthesis production term was added to the mass balance equations for PHD2 and HIF1α in the model. The simulated curves represent both the synthesis of HIF1α and its hydroxylation by increasing amounts of PHD2. As the in vivo levels of PHD2 relative to HIF1α are yet unknown experimentally and dependent on cell type, computationally we tested a six order of magnitude range in ratios to cover a significantly wide spectrum, and to characterize all outputs. At very high ratios of PHD2 to HIF1α synthesis (>10:0.1), all HIF1α becomes hydroxylated within several hours. The effect on hydroxylation using closer synthesis ratios is shown (Fig. 3A). Synthesis ratio refers to the ratio of the values for kinetic parameters, $k_{prod,HIF1\alpha}$ and $k_{prod,PHD2}$, for model cases 1 and 2, or $k'_{prod,HIF1\alpha}$ and $k'_{prod,PHD2}$, for model case 3. As the PHD2:HIF1α ratio decreases, unhydroxylated HIF1α accumulates (Fig. 3A). At very low ratios, there is a single peak of HIF1α near 10–12 h, with elevated HIF1α levels beyond 72 h; the synthesis ratio 0.001:0.1 demonstrates this (Fig. 3A). At intermediate values, where the synthesis rates approach each other within ten-fold magnitude, a second peak in $[HIF1\alpha]_{unhydroxylated}$ is present between ~48 and 60 h (Fig. 3A).

In vivo, systems can adapt to chronic conditions, decreasing HIF1α expression within days of hypoxic exposure. A balance of HIF1α and PHD2 synthesis is a possible contributing mechanism. The model predicts that unhydroxylated HIF1α accumulation decreases following PHD2 synthesis of several hours, allowing adaptation to hypoxia, and a new threshold for response to acute hypoxic stimulus within days (Fig. 3A and B). Correspondingly, a local minimum in $[HIF1\alpha]_{hydroxylated}$:$[HIF1\alpha]_{total}$ is present between 3.5 and 10 h of hypoxia, at the same PHD2:HIF1α synthesis ratios (Fig. 3C). Notably, as more PHD2 is produced after 8–12 h, the amount of unhydroxylated HIF1α increases relative to the amount of PHD2 (Fig. 3D), and the efficacy (defined by $[HIF1\alpha_{hydroxylated}]$/[PHD2]) of PHD2 in hydroxylating HIF1α decreases.

3.2. Comparison with experimental data

To help confirm if the model represents well the biological system, model output was compared to available experimental data on relative protein levels of HIF1α and PHD2 during chronic hypoxia. The computational synthesis terms accurately approximate the HIF1α and PHD2 synthesis observed in experiments (Fig. 3E–H). The trendlines for HIF1α synthesis (Fig. 3E) and PHD2 synthesis (Fig. 3F) follow those from in vitro experiments with HEK293 cells exposed to chronic hypoxia of 1% O_2 [5]. Notably, PHD2 and HIF1α expression are compared in the model and experiments under hypoxic conditions (Fig. 3E and F). The model's initial normoxic values of PHD2 and HIF1α were set as 1 μM (Fig. 3A and B), a 1:1 ratio, and changes in protein levels are relative. Actual in vivo protein levels in normoxia vary by cell type; and the chronic hypoxia model is far more sensitive to PHD2:HIF1α synthesis ratios than initial protein levels.

Fig. 3. Quantitative effect of PHD2 and HIF1α synthesis on HIF1α hydroxylation. For 2A, 2B, 2E, and 2F, the *y*-axis values are normalized to the maximum concentration or protein levels for each set of synthesis kinetic parameters. PHD2:HIF1α synthesis in (A) and (B) and SR in (E) and (F) refer to synthesis rates $k_{prod,PHD2}$:$k'_{prod,HIF1\alpha}$, (Eqs. (A1.3) and (A2.2)). (A) Model results showing the time course of HIF1α accumulation as a function of PHD2:HIF1α synthesis during hypoxic exposure of 0 to 72 h. See Supplemental Fig. 1A for the theoretical cases of no synthesis and HIF1α synthesis without PHD2 synthesis. (B) Model predictions of PHD2 expression as a function of PHD2:HIF1α synthesis and hypoxia. (C) Model results show the amount of hydroxylated [HIF1α] per total [HIF1α] for the four different sets of PHD2 and HIF1α synthesis rates. Values are normalized to 1, the maximum $[HIF1\alpha]_{hydroxylated}/[HIF1\alpha]_{total}$, for all simulations. (D) Model results for unhydroxylated [HIF1α] per [PHD2], at different PHD2:HIF1α synthesis rates normalized to the maximum $[HIF1\alpha]_{unydroxylated}/[PHD2]$ found for each set of rate parameters. (E and F) Comparison of model results with experimental data. Time t_o represents the start time of experimental data collection, a time greater than 0 and less than 4 h. For the model, the equivalent estimated time was taken as 3 h, a time after any transient hypoxic response. The model qualitatively agrees with the experimental trends shown in human embryonic kidney HEK293 cells [5] for HIF1α (E) and PHD2 (F) protein levels. Experimental comparisons of the model using alternate synthesis terms are shown in Supplemental Fig. 3. (G) The model was compared to experimental data on relative PHD2 expression at different oxygen levels producing the same amount of hydroxylation activity, after 1 h of hypoxia [5]. For the first model data points, the initial concentration of PHD2 of 0.15 μM at 1% O_2 was determined by finding what concentration at 2% O_2 produced approximately half the hydroxylation activity at 20% O_2, as found experimentally [5]. The model results were then scaled so that the PHD2 expression value at 1% corresponded to 2. Model results for $[PHD2]_0 = 1$ μM at 1% are also shown, without scaling. (H) Experimental data on relative PHD2 expression in chronic hypoxia, across a range of cell types [32], is compared to possible model outputs using different parameter values.

While the kinetic terms and the equation function could have been fit to experimental data, this would eliminate its capability of representing many different conditions and limit it to the specific experiment detailed in the comparison. Model Case 2, based on assumption of changes in PHD2 synthesis rate at 24 h, fit the in vitro PHD data most closely. However, the saturation

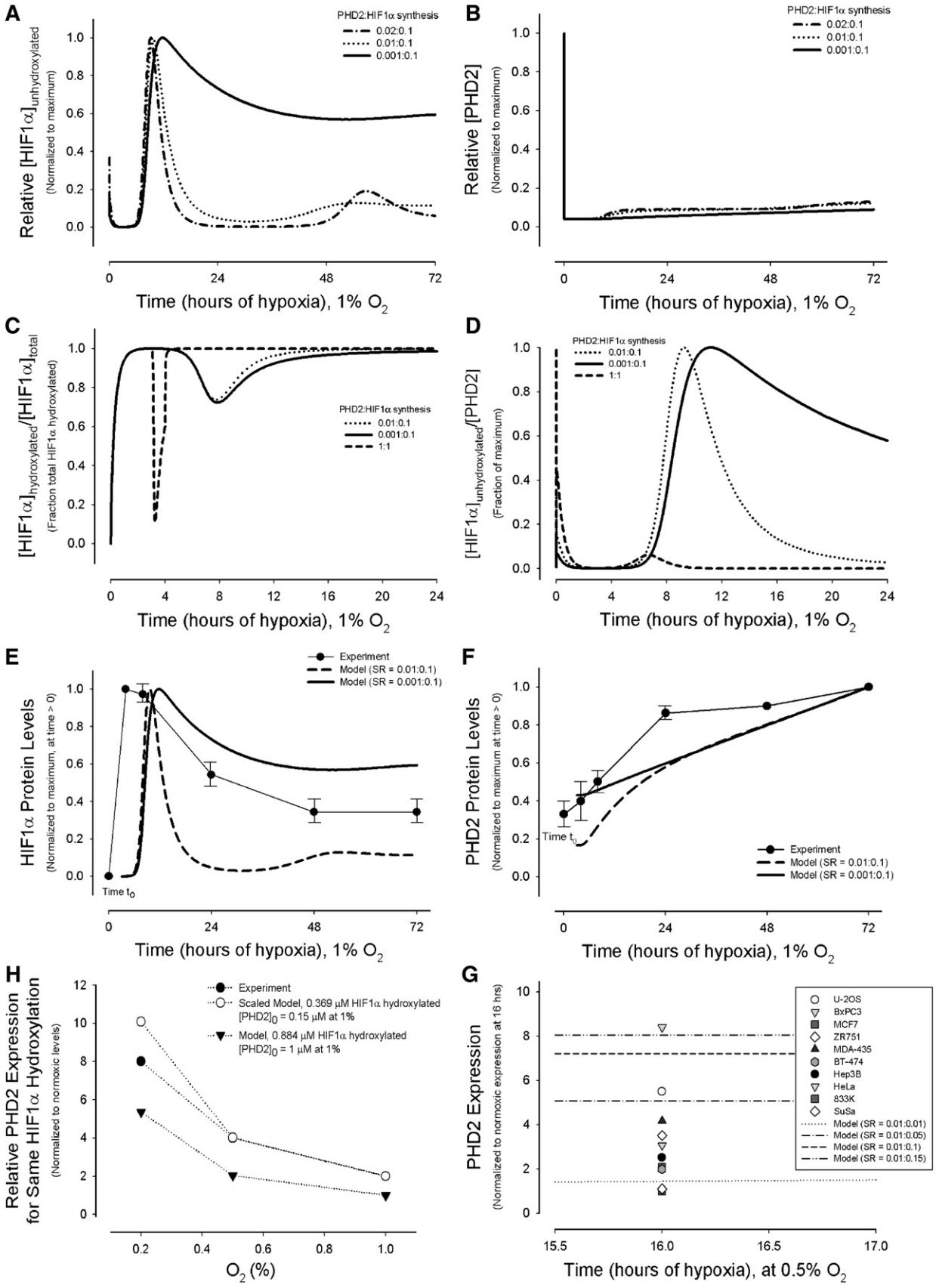

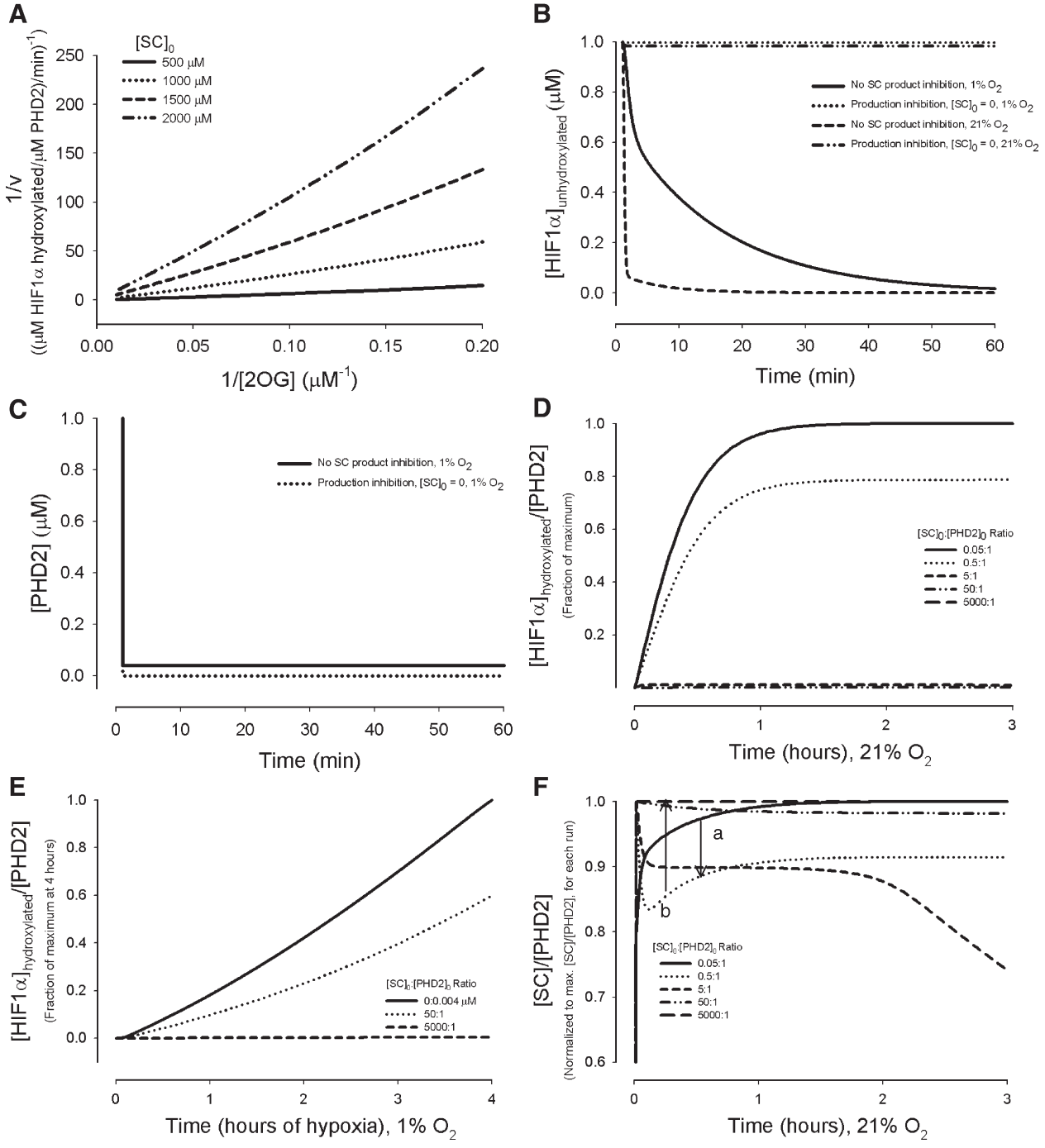

Fig. 4. Quantitative effect of succinate concentrations on HIF1α hydroxylation in normoxia (A), (B) and (D) and hypoxia (B), without synthesis of PHD2 or HIF1α. (A) The model reproduces competitive inhibition of PHD2 by succinate with respect to 2-oxoglutarate, as found in experiments [53]. If the lines are extended to zero (infinite concentrations of 2OG limit this calculation), they intersect near the y-axis. For this calculation, the K_m value used for Fe^{2+} was 0.03 μM [74], and for 2OG, was 1 μM [53], for consistency with the compared reciprocal plots [53]. $[Fe^{2+}]_0 = 5$ μM. Other kinetic parameters were kept as default values [30]. (B) HIF1α levels during transient hypoxic or normoxic conditions, with and without SC production inhibition. (C) PHD2 levels during transient hypoxia, with and without SC product inhibition. (D) Initial succinate levels affect the dynamics of HIF1α concentrations, by altering the last two steps in PHD2 hydroxylation. Values are normalized to the maximum $[HIF1\alpha]_{hydroxylated}$:[PHD2] ratio at 24 h. (E) [HIF1α] to [PHD2] ratios during the first 4 h of hypoxia, and the effects of changing $[SC]_0$:$[PHD2]_0$, without HIF1α or PHD2 synthesis. Values are normalized to the maximum $[HIF1\alpha]_{hydroxylated}$:[PHD2] ratio at 4 h. (F) Succinate to PHD2 ratios as a function of time and initial concentrations. Below a $[SC]_0$:$[PHD2]_0$ ratio of 0.05:1, the curve for $[SC]_0$:$[PHD2]_0$ follows saturation kinetics (a). Above this ratio, there is a minimum present (b). As the initial concentration ratios increase above 5:1, the [SC]/[PHD2] ratio becomes approximately constant.

and oxygen-dependency of PHD2 and HIF1α synthesis in Case 3 offered a better representation of the underlying biology (Eqs. (A1.3) and (A2.2)), and this case was used as the default model. The value of $k'_{prod,HIF1\alpha} = 0.1\ h^{-1}$ was chosen throughout the Figures using Case 3, as this was the rate that approximated experimental curves (Fig. 3E), and it was low enough to give visibly distinct changes in $[HIF1\alpha]_{unhydroxylated}$ when compared with the range of PHD2 synthesis rates explored (Fig. 3F). As a

second validation, the model's relative level of PHD2 expression required to produce the same degree of HIF1α hydroxylation during different levels of transient hypoxia agrees well with experiments (Fig. 3G). The model also was tested to ensure that it could account for experimentally observed PHD2 induction across numerous cell lines during 16 h of hypoxic exposure (0.5%) (Fig. 3H). Qualitatively, the model agrees also with the findings that hypoxic preconditioning (cultured in 5% O_2 for 4 weeks) of mouse clonal hippocampal HT22 cells exposed to 0.5% O_2 leads to increased HIF1α, at an expression level lower than cells cultured in normoxia and then exposed to 0.5% O_2 [1]. The model might predict this to be the case, as the normoxic levels of HIF1α approach zero within an hour [30], while the hypoxic levels reach a new relative minimum HIF1α level after 24 h (Fig. 3A), at the same time PHD2 levels remain elevated (Fig. 3B). Recent in vivo experiments have also confirmed the hypoxic induction of HIF1α and PHD2, and lead to hypotheses about PHD2's protective role in hypoxic preconditioning [6].

3.2.1. Succinate product inhibition

There are several mechanisms by which succinate (SC), and the catalyst for its oxidative dehydrogenation, the enzyme succinate dehydrogenase (SDH), may interfere in the PHD2 hydroxylation of HIF1α, as discussed below. We first represented succinate through product inhibition of 2-oxoglutarate binding to PHD2, and hence inhibition of PHD2 hydroxylation of HIF1α. Results are shown in Figs. 4 and 5. Fig. 4 shows the cases of no PHD2 or HIF1α synthesis. Fig. 4A, a double reciprocal plot, is provided to show that product inhibition represented in the model can qualitatively reproduce experimental results [53]. With SC production inhibition represented in the model, there is an increase in unhydroxylated HIF1α (Fig. 4B) and decrease in free PHD2 levels (Fig. 4C) compared to transient conditions without succinate product inhibition. As expected in product inhibition, at high initial succinate to PHD2 ratios (~5:1), the amount of HIF1α hydroxylated per PHD2 drops precipitously, in normoxia (Fig. 4D) and acute hypoxia (Fig. 4E). This is in qualitative agreement with recent in vitro studies on HEK 293T cells, showing addition of SC inhibited hydroxylation.

Depending on the ratio of initial SC to PHD2 levels, the temporal change in the normalized [SC]:[PHD2] ratio follows different shaped curves, as a function of the kinetic parameters in normoxia (Fig. 4F). The shape of the curve could be of interest, for detailed kinetic understanding of the effects of succinate metabolism and feedback on the HIF1α pathway. For ratios below 0.5:1, a saturation curve with no minimum is present (point a), while as the ratio increases to 0.5:1, a minimum ratio occurs shortly after the reaction begins (point b). At the higher initial concentration ratio of 5:1, beyond ~2 h of total reaction time, the [SC]:[PHD2] ratio steadily decreases. However, as the ratio increases further, this drop is replaced by the relatively constant maximum values shown.

Elevated succinate levels are most likely to be present during chronic hypoxia, such as in cancerous tissue, benign paraganglio-

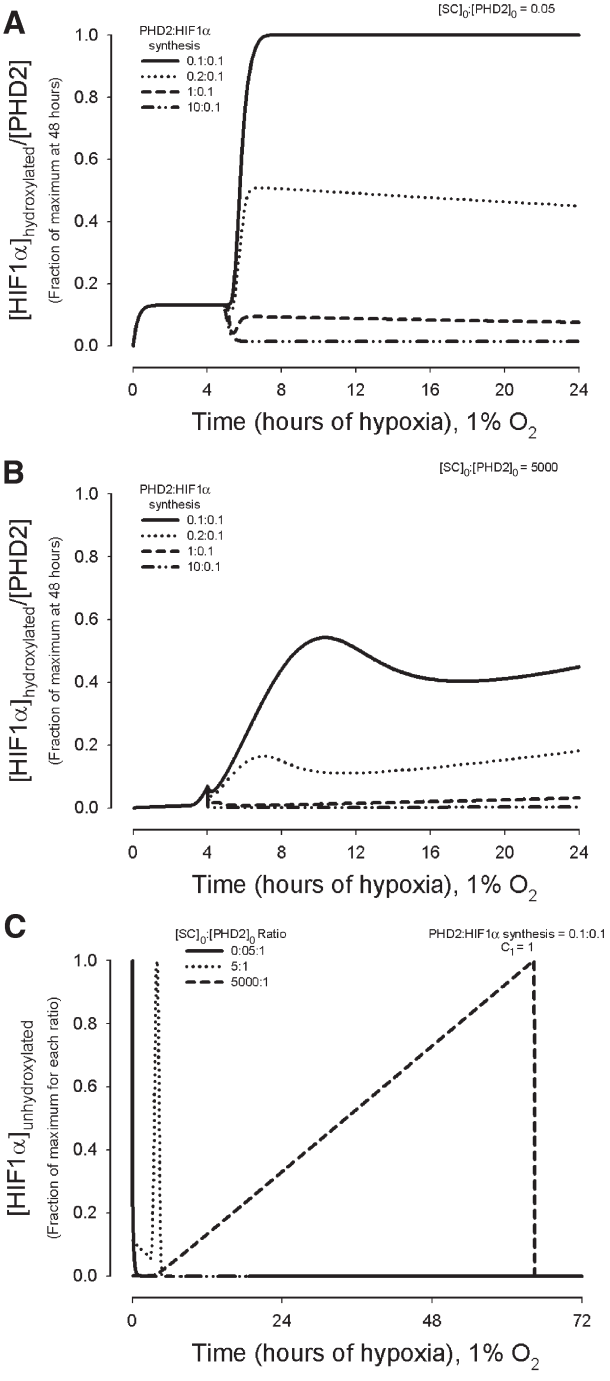

Fig. 5. Combined effects of succinate product inhibition, PHD2 synthesis, and HIF1α synthesis leads first to changing levels of $[HIF1α]_{hydroxylated}$/[PHD2], which eventually become linear over time. This linearly as time approaches infinity is predicted to result from a balance between hydroxylation and succinate inhibiting PHD2 hydroxylation, and reaching a maximum of PHD2 and HIF1α production, inherent in the model synthesis terms. In (A) and (B), values are normalized to the maximum $[HIF1α]_{hydroxylated}$:[PHD2] ratio at 48 h, for SR=0.1:0.1. (A) Results for $[PHD2]_0$=1; C_1=1; $[SC]_0$=0.5 μM. (B) Results for $[PHD2]_0$=1; C_1=1; $[SC]_0$=5000 μM, where one peak is prominent. (C) Unhydroxylated [HIF1α], an estimate of HIF1α protein accumulation, at different concentration ratios of $[SC]_0$:$[PHD2]_0$. The time step used in (C) was 0.5 min; the peaks in $[HIF1α]_{unhydroxylated}$ for the $[SC]_0$:$[PHD2]_0$=0.5:1 and 5000:1 last for ~1 min. The ratios of $[SC]_0$:$[PHD2]_0$ were chosen to represent possible ratios found in vivo in cells without a SDH or mitochondrial deficiency ($[SC]_0$:$[PHD2]_0$=0.5:1 and 5:1), as well as the extreme in vitro conditions used to mimic SDH deficiency ($[SC]_0$:$[PHD2]_0$=5000:1). For each value, the predicted time course of HIF1α hydroxylation is distinct and highly dependent on relative SC concentrations.

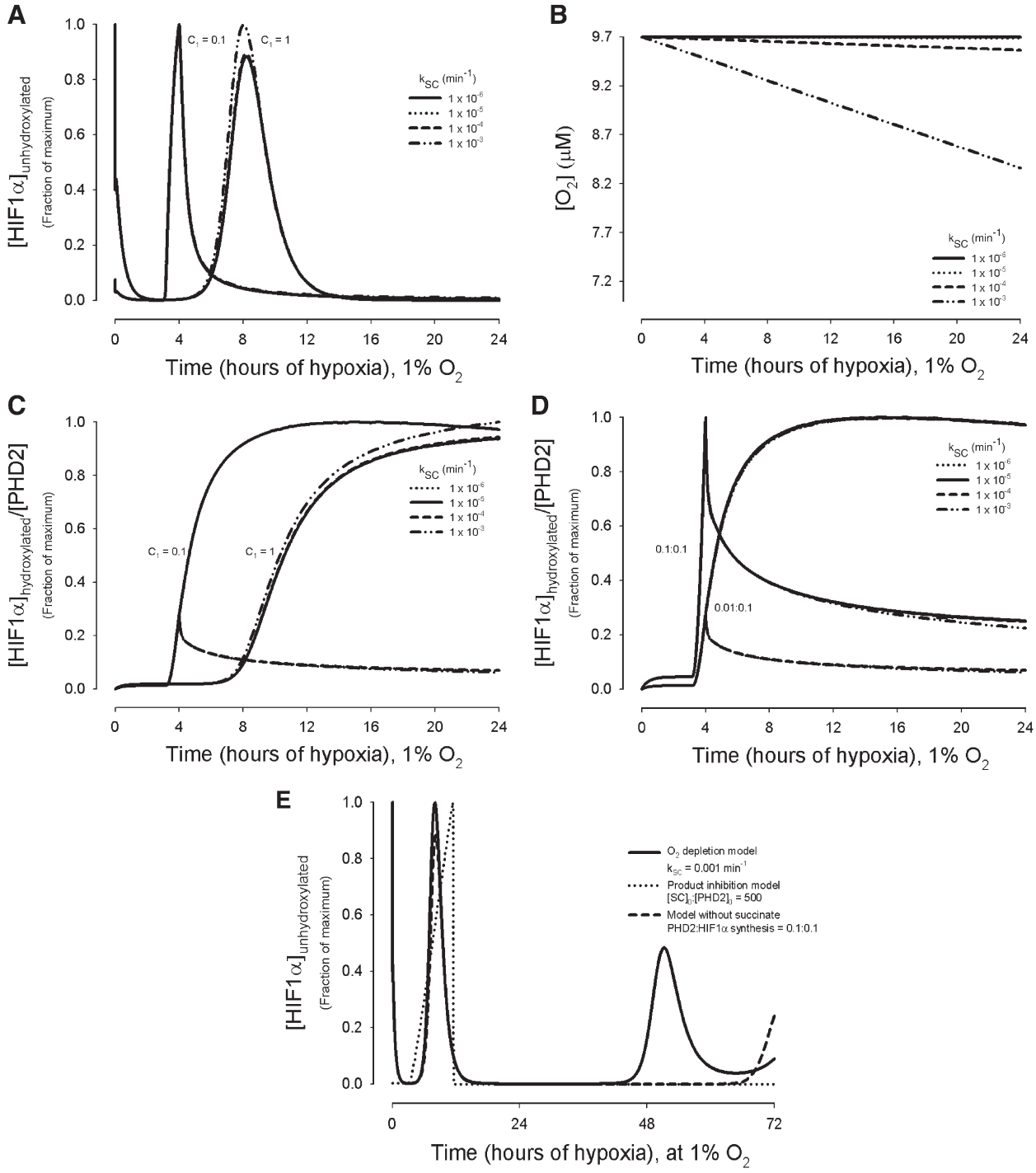

Fig. 6. Succinate may affect metabolism, independent of PHD2. This is represented in the model by succinate levels signaling decreased oxygen availability, rather than inhibiting PHD2 hydroxylation. For Fig. 5A–D, a PHD2: HIF1α synthesis ratio of 0.1:0.1 was used. For 5A, 5C, and 5D, *y*-axis parameters are normalized to the maximum value for each synthesis parameter set. (A) Amount of unhydroxylated HIF1α present in chronic hypoxia at different values of the kinetic constant k_{SC}. (B) Changes in oxygen level are represented as a function of succinate concentration through the kinetic constant k_{SC}. $[O_2]=9.7\ \mu M \cong 1\%\ O_2$. Also see Eq. (A6). (C) $[HIF1\alpha]_{hydroxylated}$:[PHD2] ratios as a function of k_{SC}. (D) $[HIF1\alpha]_{hydroxylated}$:[PHD2] ratios as a function of k_{SC}, for varying values of PHD2:HIF1α synthesis rates. (E) Relative $[HIF1\alpha]_{unhydroxylated}$ over 3 days of hypoxia. Three models are compared: O_2 depletion as a function of succinate (shown for a representative k_{SC} value of 0.001 min^{-}super ^{1}); PHD2 hydroxylation production inhibition by succinate, with initial concentration ratio of $[SC]_0:[PHD2]_0=500$; and the model with synthesis and the assumption of no succinate effects.

mas or mitochondrial myopathic muscle. Fig. 5A and B show the effect of succinate production inhibition on the hydroxylation reaction, where HIF1α synthesis and HIF1-dependent PHD2 synthesis are present, beginning after 3 and 4 h, respectively. At $[SC]_0=0.05\ \mu M$, a distinct change in $[HIF1\alpha_{hydroxylated}]$:[PHD2] occurs, shortly following the onset of PHD2 synthesis (Fig. 5A). The relative amount of PHD2 synthesized compared to HIF1α determines whether this change is an increase or decline (Fig. 5A). At this concentration of succinate, a maximum or minimum in $[HIF1\alpha]_{hydroxylated}$:[PHD2] is reached without the presence of a

pronounced peak. At higher initial succinate concentrations, a prominent peak arises for the same PHD2 to HIF1α synthesis rates; an example is shown in Fig. 5, where $[SC]_0 = 5000$ μM, a maximum concentration used in vitro assays to mimic conditions of SDH deficiency [23]. Looking at $[HIF1\alpha]_{unhydroxylated}$ alone shows how an initial succinate concentration of 5000 μM can delay the peak accumulation of HIF1α by days (Fig. 5C). During the depicted chronic hypoxia (1% O_2), free PHD2 is being bound by increasing concentrations of unhydroxylated HIF1α as well as succinate.

3.3. Succinate affecting hydroxylation, without PHD2 product inhibition

Succinate accumulation could possibly trigger a change in hydroxylation by signaling a change in TCA cycle and need for oxygen, independent of product inhibition and through an unknown mechanism. One way of modeling this potential change is by altering the oxygen availability as a function of succinate production, and introducing the kinetic term k_{SC} (Eq. (A6)). Fig. 6 shows the potential effect of succinate, where it acts not by product inhibition, but as a distinct low oxygen signaling molecule. Using initial values of $[SC]_0 = 0.05[PHD2]_0$, the effect on hydroxylation by changing k_{SC} appears minimal (Fig. 6A). Corresponding changes in oxygen are shown for these k_{SC} values (Fig. 6B).

However, when the PHD2:HIF1α synthesis rate ratio and the dependency of the rates on oxygen is varied, the effect of succinate as an oxygen signaling molecule is profound. For all increasing PHD2:HIF1α synthesis ratios where there was succinate product inhibition, the fraction of $[HIF1\alpha]_{hydroxylated}$:[PHD2] continually decreased (Fig. 5A and B). Where succinate is represented as a distinct low oxygen signaling molecule, changing values in the PHD2 and HIF1α synthesis rates can alter the response to succinate. This is achieved by altering the C_1 constant (from Table 3, Case 3) as shown in Fig. 6C, or the PHD2:HIF1α synthesis ratios (Fig. 6D). For a C_1 value of 0.1, a k_{SC} term above 10^{-4} leads to a peak of $[HIF1\alpha]_{hydroxylated}$:[PHD2] at 4 h, whereas k_{SC} values below, this show $[HIF1\alpha]_{hydroxylated}$:[PHD2] reaching a gradual maximum near 8 h (Fig. 6C). For a 0.1:0.1 ratio of PHD2:HIF1α synthesis the greatest fraction of $[HIF1\alpha]_{hydroxylated}$:[PHD2] is at 4 h for all k_{SC} terms; ratios below or above this value lead to peak that is dependent on k_{SC} values (Fig. 6D). The $[HIF1\alpha]_{hydroxylated}$:[PHD2] values eventually reach a steady-state under all conditions.

The effect of the oxygen depletion model on the relative amount of unhydroxylated HIF1α is notable. Compared to synthesis alone, it leads to a more pronounced, earlier peak whereas increasing succinate concentrations in the product inhibition model dampens any oscillations and attenuates peaks in HIF1α expression (Fig. 6E and Supplemental Fig. 3).

3.4. Adaptation and maladaptation to prolonged hypoxia

Another benefit of the computational model is that situations of specific knockouts can be explored, where they may be impossible or difficult in vivo. Here we tested the effects on adaptation to chronic hypoxia from very high PHD2:HIF1α synthesis ratios (Fig. 3A and B), HIF1α synthesis alone (data not shown), and independent alternations in succinate concentrations ([Fig. 4]). In chronic hypoxic conditions, if PHD2 is not synthesized and there is no succinate product inhibition, the accumulation of unhydroxylated HIF1 would be continuous. However, succinate as product inhibitor or a hypoxic signaling molecule may alter the effect of overproduction of HIF1α vs. PHD2 production (Fig. 6E and Supplemental Fig. 3).

4. Discussion

Chronic hypoxia is found in prolonged exercise, and disease conditions, including cancer, ischemia and chronic infection. Here we show how three compound feedback loops present in hypoxic conditions can determine the extent of HIF1α hydroxylation, after exposure to more than 3 h of low oxygen levels. Combined HIF1α synthesis, PHD2 synthesis, and succinate product inhibition dictate the relative protein levels of HIF1α present in a cell, and regulate a robust response to hypoxia. This response, which lowers the relative HIF1α after 6 to 8 h (Figs. 3A and 6E; Supplemental Fig. 3) allows adaptation to hypoxia and readies the system for a rapid response to acute hypoxic stimulus.

Several hypotheses exist as to how succinate, and its oxidizing enzyme, succinate dehydrogenase (SDH, also known as mitochondria complex II in electron transport), affect adaptation to chronic hypoxia. One possibility is through the accumulation of reactive oxygen species (ROS) when mitochondria complexes are damaged (e.g., by a SDH mutation). Another theory is that a blocked TCA cycle leads to succinate accumulation, which decreases the PHD2 hydroxylation reaction [23,33,54]. Both mechanisms could lead to stabilization of the HIF1α protein and accumulation of HIF1 [54–56]. Here we showed succinate's effect on product inhibition in the hydroxylation reaction ([Fig. 4]). Succinate levels, as measured by succinate dehydrogenase inhibition, affect HIF1α hydroxylation without the presence of redox stress [54], which complements a model of succinate product inhibition. Some studies have also shown that mitochondrial electron-transfer pathways are not needed to induce HIF1 activation or oxygen sensing [57].

On the other hand, a number of alternate hypotheses merit discussion. Hypoxic response has been shown in some studies to involve mitochondrial electron chain complexes [58], reactive oxygen species [59], and signaling through nitric oxide pathways [60]. Mitochondrial respiration and electron transfer change may limit the availability of oxygen for the PHDs [61]; however, oxidative phosphorylation has not been shown necessary for stabilization of HIF1α in hypoxia [56]. While other antioxidants show no effect on HIF1α stabilization, antioxidants that scavenge H_2O_2 prevent the stabilization of HIF1α in hypoxia [56,61]. How H_2O_2 inhibits HIF1α degradation remains unknown — possibilities include activating src kinases [55], or interfering with the redox state of iron [30,62]. Additionally, as succinate is a part of the TCA cycle, metabolic changes present in conditions like cancer, ischemia and prolonged exercise, may alter the relative levels of succinate, as well as affect pH. Further complicating analysis of the mechanism of intracellular oxygen sensing in hypoxia, nitric oxide may suppress HIF1α in hypoxic conditions (by damaging the mitochondria and leading to the release of iron and 2OG into the

cytoplasm); while in normoxia, the effect of nitric oxide may be to cause an increase in HIF1α due to competition with oxygen [63].

Limitations of the model in resolving conflicting experimental data should be mentioned. It is one hypothesis that succinate works as a product inhibitor [6,23,33,53]. Other studies have shown that TCA intermediates pyruvate and oxaloacetate bind to the 2-oxoglutarate site on the prolyl hydroxylases and inactivate HIF1α hydroxylation, whereas succinate does not have the same inactivation effect [64]. The possibility remains that the response to succinate accumulation may involve mechanisms indirectly related to HIF1α hydroxylation, as a different signal of the absence of the TCA cycle and need for increased oxygen [33]. The model showed that this alternate mechanism, acting through a decrease in oxygen as a function of succinate concentration, could have a similar effect as the succinate product inhibition on restabilizing the amount of hydroxylated HIF1α relative to PHD2 concentration (compare Fig. 5A and B with Fig. 6C and D). For the conditions used in the model, the former mechanism showed a more rapid stabilization of $[HIF1\alpha]_{unhydroxylated}$, for each PHD2:HIF1α synthesis ratio (Fig. 6E and Supplemental Fig. 3). Where PHD2 and HIF1α relative concentrations can be measured, this latter observation warrants experimental testing, in an effort to confirm one mechanism of succinate's effects.

Carbon dioxide, like succinate, is also a by-product of prolyl hydroxylation of HIF1α, formed from the reaction with 2-oxoglutarate (Eq. (A)). We leave the effect that the small changes in CO_2 concentration may have for future exploration; the overall hydroxylation reaction would also be altered by intracellular bicarbonate and pH levels, whose effects on the HIF1 pathway have been experimentally variable [65]. Also, the model incorporates the reaction of 2-oxoglutarate to form succinate, without hydroxylation, by altering the levels of succinate, availability of free iron, and the rate of hydroxylation; as relative kinetic rates become available, this reaction will be modeled independently.

Succinate was chosen as a focus for this study, as it is a product of the PHD hydroxylation reaction; its dysregulation has been studied experimentally in relation to hypoxic response and cancer [23,60,66,67]; and SDH forms complex II of the electron transport chain. Fumarate is another TCA cycle intermediate, a product of succinate reacting with SDH. Fumarate affects the HIF1α pathway by competing with 2-oxoglutarate, parallel to one known mechanism of succinate's activity [68,69]. Like succinate dehydrogenase deficiency, fumarate hydratase deficiency has been shown to lead to pseudohypoxic conditions, where HIF1α is elevated in normoxia. Both TCA enzymes have important roles in the HIF1 pathway in certain conditions, and the incorporation of fumarate as an inhibitor of PHD2 hydroxylation merits future studies.

Across cell lines, the robustness of the HIF1-dependent PHD2 feedback loop holds. The question arises, why would a positive feedback (HIF1α synthesis) and a negative feedback (PHD synthesis) on HIF1α expression be induced by the same stimuli (hypoxia)? There are several possibilities. Different PHD isoforms are induced by chronic hypoxia to various degrees [1,5], and PHD1–3 isoforms are present in different cell types at varied levels [32]. The large range of PHD2 expression profiles and hypoxic response via HIF1α expression depicted in the model may be well suited to responding to the degree and variety of hypoxic levels in the dynamic in vivo environment. A similar rationale may be applied to the use of succinate as a secondary negative feedback on hydroxylation. If succinate works by product inhibition, elevated succinate levels lead to a very distinct spike in HIF1α levels during chronic hypoxia (Fig. 6E and Supplemental Fig. 3). This effect on HIF1 expression may be of use during altered states of metabolism or malfunction of mitochondria where succinate is accumulating, to trigger a swift activation of the HIF1-regulated genetic cascade. The O_2 depletion model of succinate hints at an alternate mechanism that may accentuate a pronounced cyclic course of HIF1α (and relative PHD2 expression [6]) found during chronic hypoxia. A self-perpetuating balance between HIF1α synthesis and HIF1α degradation could make the system particularly sensitive to small alterations in oxygen levels. Adding complexity, and perhaps a fourth feedback into the HIF1 system, HIF1α has been implicated in the down-regulation of SDH, which in turn would increase succinate production and potentially block hydroxylation of HIF1α [70]. For therapeutic applications, it may be useful to explore (and perhaps exploit) the oscillations the model results show in [SC]:[PHD2] ratios in normoxia (Fig. 3B), as well as the effect of succinate on long-term hypoxia (Figs. 5 and 6; Supplemental Fig. 3).

Targeting HIF1α [71], PHD2 [72] and metabolites [68,73] therapeutically have become increasingly attractive ways of manipulating cellular hypoxic response in diseases such as critical limb ischemia and cancer. These diseases involve chronic hypoxia, where the time course of HIF1α expression differs from transient conditions. Experimentally it has been observed that HIF1α regulates itself, and PHD2 is regulated by HIF1, during chronic hypoxia. Here we developed a computational model representing these mechanisms that is able to predict the temporal expression of HIF1α during chronic hypoxia (Fig. 1B). Results show how and when the ratio of HIF1α:PHD2 synthesis has its greatest effect on HIF1α expression (Fig. 3A and C). These predictions highlight the underlying mechanism of HIF1α expression; and by exploring a range of relative synthesis ratios, the model anticipates effects of therapeutically manipulating one or both compounds.

We also represented effects of the metabolite succinate on HIF1α expression. We showed how interconnected feedback loops involving HIF1α, PHD2, and succinate together regulate a robust cellular response to hypoxic exposure of more than several hours. Understanding the mechanisms underlying how intracellular processes respond to chronic hypoxia and metabolic changes provide insight into adaptation processes. The model suggests that during days of hypoxia where there is no SDH deficiency, likely what occurs are cyclic changes in HIF1α levels, as PHD2 and HIF1α levels dynamically alter and counterbalance each other (Fig. 5E). Where there is SDH deficiency or a mitochondrial defect, if succinate inhibits hydroxylation, this cyclic expression would be dampened (Fig. 6E and Supplemental Fig. 3). In comparison, for shorter-term chronic hypoxia, such as during endurance exercise, the model represents a steep increase in HIF1α between 4 and 8 h and then leveling off to a new level of HIF1α (Fig. 3A and C), in agreement with experiments and support of the hypothesis that the mechanism underlying hypoxic preconditioning involves PHD2. These results give fundamental rationale for therapeutic design altering the HIF1 pathway, in a

temporally effective, compound-specific manner that takes into account metabolic conditions.

Acknowledgements

This work was supported by NIH 1F32HL085016-01 (A.Q.) and NIH HL079653 and NIH HL087351 (A.S.P.). The authors thank J. Pouyssegur for useful discussion.

Appendix A. Governing equations

Overall reaction sequence, incorporating the assumptions of pseudo-steady-state and bidirectionality in the binding of prolyl hydroxylase with iron, 2-oxoglutarate, oxygen and ascorbate; assumptions of pseudo-steady-state and product inhibition by succinate in the hydroxylation of HIF1α; production of HIF1α and prolyl hydroxylase; and reversibility in the ubiquitination of hydroxylated HIF1α by the VHL complex:

Parameter	Abbreviation
$(PHD2{\cdot}Fe^{2+}{\cdot}2OG{\cdot}O_2{\cdot}Asc)_{O_2\ split}$	PHD2 enzyme, following hydroxylation O_2 split refers to PHD2 using oxygen to hydroxylate HIF1α while simultaneously oxidizing 2OG to succinate

$$PHD2 + Fe^{2+} \leftrightarrow PHD2\cdot Fe^{2+} + 2OG \leftrightarrow PHD2\cdot Fe^{2+}\cdot 2OG + O_2 \leftrightarrow PHD2\cdot Fe^{2+}\cdot 2OG\cdot O_2 + Asc \leftrightarrow PHD2\cdot Fe^{2+}\cdot 2OG\cdot O_2\cdot Asc \underset{\leftarrow}{\longrightarrow} SC + CO_2 + (PHD2\cdot Fe^{2+}\cdot 2OG\cdot O_2\cdot Asc)_{O_2\ split}$$

$$HIF1\alpha \rightarrow HIF1\alpha_h \qquad (A)$$

Table 1 gives abbreviations. The 17 differential equations representing hydroxylation and ubiquitination of HIF1α were defined previously by Eqs. (10) through (26) of reference [30]. The assumption of pseudo-steady-state and bidirectionality in the binding of prolyl hydroxylase with iron, 2-oxoglutarate, oxygen and ascorbate were justified by experimental observations [76–79]. These binding reactions were assumed to follow Michaelis–Menten like kinetics, without intermediates being formed. The relationship between k_{off} and k_{on}, could then be approximated by:

$$K_m \approx K_D = \frac{k_{off}}{k_{on}}$$

The final step in the series of PHD2 binding is assumed irreversible for the hydroxylation of HIF1α by the PHD2 complex without ascorbate, $PHD2{\cdot}Fe^{2+}{\cdot}2OG{\cdot}O_2$, and with minimal reversibility for hydroxylation by the PHD2 complex with ascorbate, $PHD2_{mod} = PHD2{\cdot}Fe^{2+}{\cdot}2OG{\cdot}O_2{\cdot}Asc$, as defined by $k_{off,HIF1\alpha}$ (without consideration of SC) or $k'_{off,HIF1\alpha}$ (with SC considered).

Here we present modified equations for the mass balances of PHD2, HIF1α, and $PHD2_{mod}{\cdot}HIF1\alpha$ (Eqs. (11), (19) and (20) in reference [30]), incorporating the synthesis terms defined in Table 3. We also introduce the compound succinate, and represent two possible mechanisms of its interactions in the HIF1α pathway. In the model, succinate is included by an equation describing its concentration change with time for the case of production inhibition (Eq. (A5)) or by its effects on signaling oxygen availability (Eq. (A6)). Expect for when O_2 changes are a function of SC, changes in O_2 and CO_2 as a result of the HIF1α reactions are assumed to be negligible.

A.1. Reactions of PHD2

$$\frac{d[PHD2]}{dt} = k_{off,Fe^{2+}}\left[PHD2\cdot Fe^{2+}\right] - k_{on,Fe^{2+}}[PHD2]\left[Fe^{2+}\right] + k_{cat,Fe^{2+}}\left[PHD2\cdot Fe^{2+}\right] + q_{prod,PHD2} \qquad (A1)$$

Case 1, for all $t > t_{PHD2}$:

$$q_{prod,PHD2} = k_{prod,PHD2}\cdot q_{prod,HIF1\alpha} \qquad (A1.1)$$

Case 2, $q_{prod,PHD2}$ is defined distinctly for different times:for $t > t_{PHD2}$ and $t < 24$ h:

$$q^1_{prod,PHD2} = k'_{prod,PHD2}(t)\cdot q^2_{prod,PHD2} = k'_{prod,PHD2}(t)\cdot k_{prod,PHD2}\cdot q_{prod,HIF1\alpha} \qquad (A1.2)$$

for $t > 24$ h:

$$q^2_{prod,PHD2} = k_{prod,PHD2}\cdot q_{prod,HIF1\alpha} \qquad (A1.3)$$

Case 3 (default), for all $t > t_{PHD2}$:

$$q_{prod,PHD2} = k_{prod,PHD2}\cdot q_{prod,HIF1\alpha}$$

A.2. Reaction of $PHD2{\cdot}Fe^{2+}{\cdot}2OG{\cdot}O_2{\cdot}Asc$ ($PHD2_{mod}$) and HIFlα

Note for reactions (A2) and (A3), these equations were modified to allow reaction with an intermediate uncoupled to Asc.

$$\frac{d[HIF1\alpha]}{dt} = k'_{off,HIF1\alpha}[PHD2_{mod}\cdot HIF1\alpha][SC] - k_{on,HIF1\alpha}[PHD2_{mod}][HIF1\alpha] - k_{on,HIF1\alpha}\left[PHD2\cdot Fe^{2+}\cdot 2OG\cdot O_2\right][HIF1\alpha] + q_{prod,HIF1\alpha} \qquad (A2)$$

Cases 1 and 2, for all $t > t_{HIF1\alpha}$:

$$q_{prod,HIF1\alpha} = k_{prod,HIF1\alpha}\cdot\frac{[O_2]}{([O_2] + C_2)} \qquad (A2.1)$$

Case 3, for all $t > t_{HIF1\alpha}$:

$$q_{prod,HIF1\alpha} = k'_{prod,HIF1\alpha}\cdot\frac{[O_2]\cdot[HIF1\alpha]}{([HIF1\alpha] + C_1\cdot[O_2])} \qquad (A2.2)$$

$$\frac{d[PHD2_{mod}\cdot HIF1\alpha]}{dt} = k_{on,HIF1\alpha}[PHD2_{mod}][HIF1\alpha] + k_{on,HIF1\alpha}[PHD2\cdot Fe^{2+}\cdot 2OG\cdot O_2][HIF1\alpha] - k'_{off,HIF1\alpha}[PHD2_{mod}\cdot HIF1\alpha][SC] - k_{cat,HIF1\alpha}[PHD2_{mod}\cdot HIF1\alpha] \qquad (A3)$$

$$\frac{d[HIF1\alpha_h]}{dt} = k_{cat,HIF1\alpha}[PHD2_{mod}\cdot HIF1\alpha] \qquad (A4)$$

A.3. Reaction of SC production

$$\frac{d[\mathrm{SC}]}{\mathrm{d}t} = k_{\mathrm{on,HIF1}\alpha}[\mathrm{PHD2_{mod}}][\mathrm{HIF1}\alpha] - k'_{\mathrm{off,HIF1}\alpha}[\mathrm{PHD2_{mod}}\cdot\mathrm{HIF1}\alpha][\mathrm{SC}] \quad \text{(A5)}$$

A.4. Change in O_2 levels as a function of SC (equation used for Fig. 6) O_2 reaction binding terms remain as in [30]

$$\frac{d[\mathrm{O_2}]}{\mathrm{d}t} = -k_{\mathrm{SC}}[\mathrm{SC}] \quad \text{(A6)}$$

Appendix B. Supplementary data

Supplementary data associated with this article can be found, in the online version, at doi:10.1016/j.bbamcr.2007.07.004.

References

[1] S. Khanna, S. Roy, M. Maurer, R.R. Ratan, C.K. Sen, Oxygen-sensitive reset of hypoxia-inducible factor transactivation response: prolyl hydroxylases tune the biological normoxic set point, Free Radic. Biol. Med. 40 (2006) 2147–2154.

[2] D.D. Kline, Y.J. Peng, D.J. Manalo, G.L. Semenza, N.R. Prabhakar, Defective carotid body function and impaired ventilatory responses to chronic hypoxia in mice partially deficient for hypoxia-inducible factor 1 alpha, Proc. Natl. Acad. Sci. U. S. A. 99 (2002) 821–826.

[3] G. D'Angelo, E. Duplan, N. Boyer, P. Vigne, C. Frelin, Hypoxia up-regulates prolyl hydroxylase activity: a feedback mechanism that limits HIF-1 responses during reoxygenation, J. Biol. Chem. 278 (2003) 38183–38187.

[4] F.R. Sharp, R. Ran, A. Lu, Y. Tang, K.I. Strauss, T. Glass, T. Ardizzone, M. Bernaudin, Hypoxic preconditioning protects against ischemic brain injury, Neurorx 1 (2004) 26–35.

[5] D.P. Stiehl, R. Wirthner, J. Koditz, P. Spielmann, G. Camenisch, R.H. Wenger, Increased prolyl 4-hydroxylase domain proteins compensate for decreased oxygen levels. Evidence for an autoregulatory oxygen-sensing system, J. Biol. Chem. 281 (2006) 23482–23491.

[6] N.M. Jones, E.M. Lee, T.G. Brown, B. Jarrott, P.M. Beart, Hypoxic preconditioning produces differential expression of hypoxia-inducible factor-1alpha (HIF-1alpha) and its regulatory enzyme HIF prolyl hydroxylase 2 in neonatal rat brain, Neurosci. Lett. 404 (2006) 72–77.

[7] F.L. Powell, Functional genomics and the comparative physiology of hypoxia, Annu. Rev. Physiol. 65 (2003) 203–230.

[8] G.L. Semenza, Hydroxylation of HIF-1: oxygen sensing at the molecular level, Physiology (Bethesda) 19 (2004) 176–182.

[9] E. Berra, E. Benizri, A. Ginouves, V. Volmat, D. Roux, J. Pouyssegur, HIF prolyl-hydroxylase 2 is the key oxygen sensor setting low steady-state levels of HIF-1alpha in normoxia, EMBO J. 22 (2003) 4082–4090.

[10] K.H. Lee, E. Choi, Y.S. Chun, M.S. Kim, J.W. Park, Differential responses of two degradation domains of HIF-1alpha to hypoxia and iron deficiency, Biochimie 88 (2006) 163–169.

[11] M. Milkiewicz, O. Hudlicka, J. Verhaeg, S. Egginton, M.D. Brown, Differential expression of Flk-1 and Flt-1 in rat skeletal muscle in response to chronic ischaemia: favourable effect of muscle activity, Clin. Sci. (Lond.) 105 (2003) 473–482.

[12] R. Bos, P.J. van Diest, J.S. de Jong, P. van der Groep, P. van der Valk, E. van der Wall, Hypoxia-inducible factor-1alpha is associated with angiogenesis, and expression of bFGF, PDGF-BB, and EGFR in invasive breast cancer, Histopathology 46 (2005) 31–36.

[13] H.H. Marti, Erythropoietin and the hypoxic brain, J. Exp. Biol. 207 (2004) 3233–3242.

[14] K.S. Hewitson, C.J. Schofield, The HIF pathway as a therapeutic target, Drug Discov. Today 9 (2004) 704–711.

[15] G.L. Semenza, P.H. Roth, H.M. Fang, G.L. Wang, Transcriptional regulation of genes encoding glycolytic enzymes by hypoxia-inducible factor 1, J. Biol. Chem. 269 (1994) 23757–23763.

[16] B. Blouw, H. Song, T. Tihan, J. Bosze, N. Ferrara, H.P. Gerber, R.S. Johnson, G. Bergers, The hypoxic response of tumors is dependent on their microenvironment, Cancer Cells 4 (2003) 133–146.

[17] J.A. Garcia, HIFing the brakes: therapeutic opportunities for treatment of human malignancies, Sci. STKE 2006 (2006) pe25.

[18] C. Lundby, M. Gassmann, H. Pilegaard, Regular endurance training reduces the exercise induced HIF-1alpha and HIF-2alpha mRNA expression in human skeletal muscle in normoxic conditions, Eur. J. Appl. Physiol. 96 (2006) 363–369.

[19] T.A. Khan, F.W. Sellke, R.J. Laham, Gene therapy progress and prospects: therapeutic angiogenesis for limb and myocardial ischemia, Gene Ther. 10 (2003) 285–291.

[20] G.L. Semenza, Targeting HIF-1 for cancer therapy, Nat. Rev., Cancer 3 (2003) 721–732.

[21] G.L. Semenza, HIF-1 and tumor progression: pathophysiology and therapeutics, Trends Mol. Med. 8 (2002) S62–S67.

[22] S. Lee, E. Nakamura, H. Yang, W. Wei, M.S. Linggi, M.P. Sajan, R.V. Farese, R.S. Freeman, B.D. Carter, W.G. Kaelin Jr., S. Schlisio, Neuronal apoptosis linked to EglN3 prolyl hydroxylase and familial pheochromocytoma genes: developmental culling and cancer, Cancer Cell 8 (2005) 155–167.

[23] M.A. Selak, S.M. Armour, E.D. MacKenzie, H. Boulahbel, D.G. Watson, K.D. Mansfield, Y. Pan, M.C. Simon, C.B. Thompson, E. Gottlieb, Succinate links TCA cycle dysfunction to oncogenesis by inhibiting HIF-alpha prolyl hydroxylase, Cancer Cell 7 (2005) 77–85.

[24] K.J. O'Byrne, A.G. Dalgleish, M.J. Browning, W.P. Steward, A.L. Harris, The relationship between angiogenesis and the immune response in carcinogenesis and the progression of malignant disease, Eur. J. Cancer 36 (2000) 151–169.

[25] J. Josko, M. Mazurek, Transcription factors having impact on vascular endothelial growth factor (VEGF) gene expression in angiogenesis, Med. Sci. Monit. 10 (2004) RA89–RA98.

[26] M. Koshiji, L.E. Huang, Dynamic balancing of the dual nature of HIF-1alpha for cell survival, Cell Cycle 3 (2004) 853–854.

[27] O. Aprelikova, G.V. Chandramouli, M. Wood, J.R. Vasselli, J. Riss, J.K. Maranchie, W.M. Linehan, J.C. Barrett, Regulation of HIF prolyl hydroxylases by hypoxia-inducible factors, J. Cell. Biochem. 92 (2004) 491–501.

[28] E. Berra, D.E. Richard, E. Gothie, J. Pouyssegur, HIF-1-dependent transcriptional activity is required for oxygen-mediated HIF-1alpha degradation, FEBS Lett. 491 (2001) 85–90.

[29] Y. Pan, K.D. Mansfield, C.C. Bertozzi, V. Rudenko, D.A. Chan, A.J. Giaccia, M.C. Simon, Multiple factors affecting cellular redox status and energy metabolism modulate hypoxia-inducible factor prolyl hydroxylase activity in vivo and in vitro, Mol. Cell. Biol. 27 (2007) 912–925.

[30] A.A. Qutub, A.S. Popel, A computational model of intracellular oxygen sensing by hypoxia-inducible factor HIF1 alpha, J. Cell Sci. 119 (2006) 3467–3480.

[31] D. Ehrismann, E. Flashman, D.N. Genn, N. Mathioudakis, K.S. Hewitson, P.J. Ratcliffe, C.J. Schofield, Studies on the activity of the hypoxia-inducible-factor hydroxylases using an oxygen consumption assay, Biochem. J. 401 (2007) 227–234.

[32] R.J. Appelhoff, Y.M. Tian, R.R. Raval, H. Turley, A.L. Harris, C.W. Pugh, P.J. Ratcliffe, J.M. Gleadle, Differential function of the prolyl hydroxylases PHD1, PHD2, and PHD3 in the regulation of hypoxia-inducible factor, J. Biol. Chem. 279 (2004) 38458–38465.

[33] P.J. Pollard, J.J. Briere, N.A. Alam, J. Barwell, E. Barclay, N.C. Wortham, T. Hunt, M. Mitchell, S. Olpin, S.J. Moat, I.P. Hargreaves, S.J. Heales, Y.L. Chung, J.R. Griffiths, A. Dalgleish, J.A. McGrath, M.J. Gleeson, S.V. Hodgson, R. Poulsom, P. Rustin, I.P. Tomlinson, Accumulation of Krebs cycle intermediates and over-expression of HIF1alpha in tumours which result from germline FH and SDH mutations, Hum. Mol. Genet. 14 (2005) 2231–2239.

[34] X. Yao, A.M. Pajor, The transport properties of the human renal Na(+)-dicarboxylate cotransporter under voltage-clamp conditions, Am. J. Physiol., Cell Physiol. 279 (2000) F54–F64.

[35] W.V. Howes, F.B. Mc, Isocitrate lyase and malate synthase in *Pseudomonas indigofera*. II. Enzyme changes during the phase of adjustment and the early exponential phase, J. Bacteriol. 84 (1962) 1222–1227.

[36] N.I. Fedotcheva, A.P. Sokolov, M.N. Kondrashova, Nonezymatic formation of succinate in mitochondria under oxidative stress, Free Radic. Biol. Med. 41 (2006) 56–64.
[37] J.R. Tuckerman, Y. Zhao, K.S. Hewitson, Y.M. Tian, C.W. Pugh, P.J. Ratcliffe, D.R. Mole, Determination and comparison of specific activity of the HIF-prolyl hydroxylases, FEBS Lett. 576 (2004) 145–150.
[38] L.G. Griffith, M.A. Swartz, Capturing complex 3D tissue physiology in vitro, Nat. Rev., Mol. Cell Biol. 7 (2006) 211–224.
[39] E. Metzen, M. Wolff, J. Fandrey, W. Jelkmann, Pericellular PO2 and O2 consumption in monolayer cell cultures, Respir. Physiol. 100 (1995) 101–106.
[40] J.W. Allen, S.N. Bhatia, Formation of steady-state oxygen gradients in vitro: application to liver zonation, Biotechnol. Bioeng. 82 (2003) 253–262.
[41] V.K. Kutala, N.L. Parinandi, R.P. Pandian, P. Kuppusamy, Simultaneous measurement of oxygenation in intracellular and extracellular compartments of lung microvascular endothelial cells, Antioxid. Redox Signal. 6 (2004) 597–603.
[42] E.O. Pettersen, L.H. Larsen, N.B. Ramsing, P. Ebbesen, Pericellular oxygen depletion during ordinary tissue culturing, measured with oxygen microsensors, Cell Prolif. 38 (2005) 257–267.
[43] M. Guppy, P. Leedman, X. Zu, V. Russell, Contribution by different fuels and metabolic pathways to the total ATP turnover of proliferating MCF-7 breast cancer cells, Biochem. J. 364 (2002) 309–315.
[44] R.D. Guzy, P.T. Schumacker, Oxygen sensing by mitochondria at complex III: the paradox of increased reactive oxygen species during hypoxia, Exp. Physiol. 91 (2006) 807–819.
[45] D.P. Jones, Intracellular diffusion gradients of O2 and ATP, Am. J. Physiol. 250 (1986) C663–C675.
[46] P.G. Arthur, C.T. Ngo, P. Moretta, M. Guppy, Lack of oxygen sensing by mitochondria in platelets, Eur. J. Biochem. 266 (1999) 215–219.
[47] W.L. Rumsey, C. Schlosser, E.M. Nuutinen, M. Robiolio, D.F. Wilson, Cellular energetics and the oxygen dependence of respiration in cardiac myocytes isolated from adult rat, J. Biol. Chem. 265 (1990) 15392–15402.
[48] M. Robiolio, W.L. Rumsey, D.F. Wilson, Oxygen diffusion and mitochondrial respiration in neuroblastoma cells, Am. J. Physiol. 256 (1989) C1207–C1213.
[49] D.P. Jones, H.S. Mason, Gradients of O2 concentration in hepatocytes, J. Biol. Chem. 253 (1978) 4874–4880.
[50] P.D. Morse II, H.M. Swartz, Measurement of intracellular oxygen concentration using the spin label TEMPOL, Magn. Reson. Med. 2 (1985) 114–127.
[51] C.L. Cioffi, X.Q. Liu, P.A. Kosinski, M. Garay, B.R. Bowen, Differential regulation of HIF-1 alpha prolyl-4-hydroxylase genes by hypoxia in human cardiovascular cells, Biochem. Biophys. Res. Commun. 303 (2003) 947–953.
[52] J.H. Marxsen, P. Stengel, K. Doege, P. Heikkinen, T. Jokilehto, T. Wagner, W. Jelkmann, P. Jaakkola, E. Metzen, Hypoxia-inducible factor-1 (HIF-1) promotes its degradation by induction of HIF-alpha-prolyl-4-hydroxylases, Biochem. J. 381 (2004) 761–767.
[53] P. Koivunen, M. Hirsila, A.M. Remes, I.E. Hassinen, K.I. Kivirikko, J. Myllyharju, Inhibition of hypoxia-inducible factor (HIF) hydroxylases by citric acid cycle intermediates: possible links between cell metabolism and stabilization of HIF, J. Biol. Chem. 282 (2007) 4524–4532.
[54] M.A. Selak, R.V. Duran, E. Gottlieb, Redox stress is not essential for the pseudo-hypoxic phenotype of succinate dehydrogenase deficient cells, Biochim. Biophys. Acta 1757 (2006) 567–572.
[55] E.L. Bell, B.M. Emerling, N.S. Chandel, Mitochondrial regulation of oxygen sensing, Mitochondrion 5 (2005) 322–332.
[56] J.K. Brunelle, E.L. Bell, N.M. Quesada, K. Vercauteren, V. Tiranti, M. Zeviani, R.C. Scarpulla, N.S. Chandel, Oxygen sensing requires mitochondrial ROS but not oxidative phosphorylation, Cell Metab. 1 (2005) 409–414.
[57] V. Srinivas, I. Leshchinsky, N. Sang, M.P. King, A. Minchenko, J. Caro, Oxygen sensing and HIF-1 activation does not require an active mitochondrial respiratory chain electron-transfer pathway, J. Biol. Chem. 276 (2001) 21995–21998.
[58] F.H. Agani, P. Pichiule, J.C. Chavez, J.C. LaManna, The role of mitochondria in the regulation of hypoxia-inducible factor 1 expression during hypoxia, J. Biol. Chem. 275 (2000) 35863–35867.
[59] R.D. Guzy, B. Hoyos, E. Robin, H. Chen, L. Liu, K.D. Mansfield, M.C. Simon, U. Hammerling, P.T. Schumacker, Mitochondrial complex III is required for hypoxia-induced ROS production and cellular oxygen sensing, Cell Metab. 1 (2005) 401–408.
[60] F.H. Agani, M. Puchowicz, J.C. Chavez, P. Pichiule, J. LaManna, Role of nitric oxide in the regulation of HIF-1alpha expression during hypoxia, Am. J. Physiol., Cell Physiol. 283 (2002) C178–C186.
[61] T. Hagen, C.T. Taylor, F. Lam, S. Moncada, Redistribution of intracellular oxygen in hypoxia by nitric oxide: effect on HIF1alpha, Science 302 (2003) 1975–1978.
[62] J. Pouyssegur, F. Mechta-Grigoriou, Redox regulation of the hypoxia-inducible factor, Biol. Chem. 387 (2006) 1337–1346.
[63] A.V. Kozhukhar, I.M. Yasinska, V.V. Sumbayev, Nitric oxide inhibits HIF-1alpha protein accumulation under hypoxic conditions: implication of 2-oxoglutarate and iron, Biochimie 88 (2006) 411–418.
[64] H. Lu, C. Dalgard, A. Mohyeldin, T. McFate, A.S. Tait, A. Verma, Reversible inactivation of HIF-1 prolyl hydroxylases allows cell metabolism to control basal HIF-1, J. Biol. Chem. 280 (2005) 41928–41938.
[65] C. Willam, C. Warnecke, J.C. Schefold, J. Kugler, P. Koehne, U. Frei, M. Wiesener, K.U. Eckardt, Inconsistent effects of acidosis on HIF-alpha protein and its target genes, Pflugers Arch. 451 (2006) 534–543.
[66] M.C. Tissot van Patot, J. Bendrick-Peart, V.E. Beckey, N. Serkova, L. Zwerdlinger, Greater vascularity, lowered HIF-1/DNA binding, and elevated GSH as markers of adaptation to in vivo chronic hypoxia, Am. J. Physiol., Lung Cell. Mol. Physiol. 287 (2004) L525–L532.
[67] S.M. Baby, A. Roy, S. Lahiri, Role of mitochondria in the regulation of hypoxia-inducible factor-1alpha in the rat carotid body glomus cells, Histochem. Cell Biol. 124 (2005) 69–76.
[68] E.D. MacKenzie, M.A. Selak, D.A. Tennant, L.J. Payne, S. Crosby, C.M. Frederiksen, D.G. Watson, E. Gottlieb, Cell-permeating alpha-ketoglutarate derivatives alleviate pseudohypoxia in succinate dehydrogenase-deficient cells, Mol. Cell. Biol. 27 (2007) 3282–3289.
[69] A. King, M.A. Selak, E. Gottlieb, Succinate dehydrogenase and fumarate hydratase: linking mitochondrial dysfunction and cancer, Oncogene 25 (2006) 4675–4682.
[70] P.L. Dahia, K.N. Ross, M.E. Wright, C.Y. Hayashida, S. Santagata, M. Barontini, A.L. Kung, G. Sanso, J.F. Powers, A.S. Tischler, R. Hodin, S. Heitritter, F. Moore, R. Dluhy, J.A. Sosa, I.T. Ocal, D.E. Benn, D.J. Marsh, B.G. Robinson, K. Schneider, J. Garber, S.M. Arum, M. Korbonits, A. Grossman, P. Pigny, S.P. Toledo, V. Nose, C. Li, C.D. Stiles, A HIF1alpha regulatory loop links hypoxia and mitochondrial signals in pheochromocytomas, PLoS Genet. 1 (2005) 72–80.
[71] S. Rajagopalan, J. Olin, S. Deitcher, A. Pieczek, J. Laird, P.M. Grossman, C.K. Goldman, K. McEllin, R. Kelly, N. Chronos, Use of a constitutively active hypoxia-inducible factor-1alpha transgene as a therapeutic strategy in no-option critical limb ischemia patients: phase I dose-escalation experience, Circulation 115 (2007) 1234–1243.
[72] R. Natarajan, F.N. Salloum, B.J. Fisher, E.D. Ownby, R.C. Kukreja, A.A. Fowler, Activation of hypoxia inducible factor-1 via prolyl-4 hydoxylase-2 gene silencing attenuates acute inflammatory responses in post-ischemic myocardium, Am. J. Physiol, Heart Circ. Physiol., in press.
[73] G.L. Semenza, HIF-1 mediates the Warburg effect in clear cell renal carcinoma, J. Bioenerg. Biomembranes, in press
[74] M. Hirsila, P. Koivunen, L. Xu, T. Seeley, K.I. Kivirikko, J. Myllyharju, Effect of desferrioxamine and metals on the hydroxylases in the oxygen sensing pathway, FASEB J. 19 (2005) 1308–1310.
[75] B. Gonzalez-Flecha, B. Demple, Homeostatic regulation of intracellular hydrogen peroxide concentration in aerobically growing *Escherichia coli*, J. Bacteriol. 179 (1997) 382–388.
[76] M. Hirsila, Medical Biochemistry and Molecular Biology, University of Oulu, Oulu, Finland, 2004, p. 99.
[77] J. Myllyharju, K.I. Kivirikko, Characterization of the iron- and 2-oxoglutarate-binding sites of human prolyl 4-hydroxylase, EMBO J. 16 (1997) 1173–1180.
[78] R. Myllyla, L. Tuderman, K.I. Kivirikko, Mechanism of the prolyl hydroxylase reaction. 2. Kinetic analysis of the reaction sequence, Eur. J. Biochem. 80 (1977) 349–357.
[79] L. Tuderman, R. Myllyla, K.I. Kivirikko, Mechanism of the prolyl hydroxylase reaction: 1. Role of co-substrates, Eur. J. Biochem. 80 (1977) 341–348.